Virtual age models with time-dependent covariates: A framework for simulation, parametric inference and quality of estimation

Léa Brenière, Laurent Doyen, Christophe Bérenguer

Virtual Age Models With Time-Dependent Covariates: A Framework for Simulation, Parametric Inference and Quality of Estimation

Léa Brenière[a,b,*], Laurent Doyen[a], Christophe Bérenguer[b]

[a] *Univ. Grenoble Alpes, CNRS, Grenoble INP[1], LJK, 38000 Grenoble, France*
[b] *Univ. Grenoble Alpes, CNRS, Grenoble INP[1], GIPSA-lab, 38000 Grenoble, France*

Abstract

A repairable system faces some failures and imperfect maintenances throughout its lifetime. If several identical and independent systems are considered together, some differences may arise between the systems, such as the geographical location or the maintenance team for example, which are constant information, or the weather conditions, which vary with time. This observed heterogeneity will influence more or less the failure process. In this paper, we include these data in a generalized virtual age model with the use of covariates. Then we estimate simultaneously the effect of the maintenances, that of the covariates, and the intrinsic wear of the systems. We also propose two simulation methods as well as a numerical estimation procedure. Then we assess the quality of the estimation of the parameters with a thorough simulation study.

Keywords: Imperfect repair, virtual age model, time-dependent covariate, failure times simulation, parametric estimation, quality of estimation

Acronyms

ABAO	As Bad As Old
AGAN	As Good As New
ARA	Arithmetic Reduction of Age
QR	Quasi Renewal
PLP	Power Law Process
MSE	Mean Squared Error

[1] Institute of Engineering Univ. Grenoble Alpes
[*] Corresponding author
Email addresses: lea.breniere@univ-grenoble-alpes.fr (Léa Brenière), laurent.doyen@univ-grenoble-alpes.fr (Laurent Doyen), christophe.berenguer@grenoble-inp.fr (Christophe Bérenguer)

Notations

$T_1, \ldots, T_n$	n first failure times of a single repairable system, with $T_0 = 0$
$N = (N_t)_{t \geq 0}$	counting process of failures
$\lambda = (\lambda_t)_{t \geq 0}$	failure intensity
$\mathcal{H}_{t^-}$	history of the failure process just before t
$h(\cdot)$	hazard rate of the first time to failure
$V_i(t),\ t \geq 0,\ i \geq 0$	virtual age at time t after i observed failures
$\mathbb{X}_t,\ t \geq 0$	time-dependent covariates at time t
$F_{i+1}(\cdot),\ i \geq 0$	conditional cumulative distribution function of T_{i+1} knowing the past of the process and of the covariates
$H(\cdot)$	cumulative hazard rate of the first time to failure: primitive integral of $h(\cdot)$ with $H(0) = 0$
$F_{i+1}^{-1}(\cdot),\ i \geq 0$	generalized inverse of $F_{i+1}(\cdot)$
$V_i^{-1}(\cdot),\ i \geq 0$	generalized inverse of $V_i(\cdot)$
$H^{-1}(\cdot)$	generalized inverse of $H(\cdot)$
L	number of constant steps of the covariates
$\tau_l,\ 0 \leq l \leq L-1$	discontinuity points of the covariates, with $\tau_0 = 0$
$\chi_l,\ 1 \leq l \leq L$	values taken by the covariates on the constant steps
$l_{(t)},\ t \geq 0$	number of the covariate step at time t, *i.e.* $l_{(t)} = \sum_{l=0}^{L-1} \mathbf{1}_{\{\tau_l \leq t\}}$
$\mathcal{T}$	fixed end of observation time of the systems
$\mathcal{L}$	log-likelihood for one observed system
$\varsigma_k,\ 0 \leq k \leq N_{\mathcal{T}^-} + L$	time either of jump of the covariate or of failure
$\ell_k,\ 0 \leq k \leq N_{\mathcal{T}^-} + L$	number of the current covariate step, *i.e.* $\ell_k = \sum_{l=0}^{L} \mathbf{1}_{\{\tau_l \leq \varsigma_k\}} = l_{(\varsigma_k)}$
$\imath_k,\ 0 \leq k \leq N_{\mathcal{T}^-} + L$	current number of failures, *i.e.* $\imath_k = \sum_{i=1}^{N_{\mathcal{T}^-}+1} \mathbf{1}_{\{T_i \leq \varsigma_k\}} = N_{\varsigma_k}$
K	$K \in \{0, \ldots, N_{\mathcal{T}^-} + L\}$ such that $\varsigma_{K+1} = T_{N_{\mathcal{T}^-}+1}$
η, β	scale and shape parameters of a PLP
ρ	efficiency parameter of a virtual age model
γ	coefficient of influence of the covariates
$\theta,\ \theta_0,\ \hat{\theta}$	a model parameter, its true value used in simulation, its estimation
$MSE(\hat{\theta}_{(M)})$	MSE of a parameter θ
$nMSE(\hat{\theta}_{(M)})$	normalized MSE of a parameter θ

1. Introduction

1.1. Context

An industrial system can face several failures and repairs throughout its whole lifetime, rather than dying with its first and last breakdown. This is the point where survival analysis becomes recurrent data analysis: we no more have a sample of the dates of death of some independent systems, but successive failure times for each system. Here, we will consider that these failure times also correspond to the repair times, *i.e.* the durations of the repairs themselves are not taken into account and are considered to be negligible.

When a repair is performed on a system, we can think of an operator only switching on again the system, without doing more. It is for example the case when a computer is rebooted after a bug or when a circuit breaker is reset after it tripped. Then the system is As Bad As Old (ABAO), since its wear is the same as just before the failure. Conversely, one could decide to replace the system with a new but identical one, *i.e.* to renew the system: then the system is As Good As New (AGAN). Some repair actions might match with one or the other situation, but in most cases, they are likely to fall in between, with a reduction of the wear of the system that does not bring it into an AGAN state. This is called imperfect maintenance or repair.

Important models dealing with imperfect maintenances are the Type I and Type II Kijima's models [1]. These models work with a quantity called the virtual age or effective age of the system. Let $T_1, \ldots, T_n$ be the n first failure times of a system, with $T_0 = 0$. At some time $t \in [T_{i-1}, T_i]$, $1 \leq i \leq n$, the system is supposed to be in the same state as an unmaintained system that never failed up to time $V_i(t)$. $V_i(t)$ is called the virtual age. For these models, Doyen and Gaudoin [2] have proposed different parametrizations in which the virtual age is reduced by a quantity depending on a scalar ρ, which corresponds to the efficiency of the maintenance. In particular, they proposed the Arithmetic Reduction of Age (ARA) models. This way of dealing with virtual age models is generalized by Doyen *et al.* [3], where other imperfect maintenance models such as the Quasi Renewal (QR) model of Wang and Pham [4] are included within the same framework. Simulation of datasets and parameter estimation are also considered. For these models, Chauvel *et al.* [5] proposed goodness-of-fit tests wih a parametric bootstrap approach. Other models were designed, generally with an estimation procedure, for example by Dauxois and Maalouf [6], Dauxois *et al.* [7], Dijoux *et al.* [8], Doyen *et al.* [9], and Peng *et al.* [10]. Some models also include preventive maintenances, as those exposed by Peng *et al.* [11], Said and Taghipour [12] and Salles *et al.* [13]. Preventive maintenances are carried out without the occurence of a failure. They can also be imperfect, which leads to additional consideration for example when optimizing the time interval between two planned preventive maintenances. Imperfect models for preventive maintenances were studied by Hu *et al.* [14], Huynh [15], Mercier and Castro [16], Mullor *et al.* [17] and Yang *et al.* [18].

Covariates are known data recording factors that have a potential influence on the failure process. In the reliability context, it can be for example the geographical location of the system, which is a constant information, or the weather conditions in which it works, which varies with time. With the growing availability of information from sensors or automatic data collecting, a new field of research has appeared to study the heterogeneity existing between apparently identical systems. Many articles deal with the addition of covariates in survival analysis. For example, Aramesh *et al.* [19], Man and Zhou [20] and Man and Zhou [21] study covariates with survival data and give an estimation procedure. The simulation of survival times under the influence of covariates is studied by Bender *et al.* [22]. The difference between constant and time-dependent covariates is discussed by Fisher and Lin [23]. Zhou *et al.* [24] provide a joint modelling where the degradation becomes a time-dependent covariate of the hard failure process.

Recurrent events data are also associated with covariates in some articles. For example,

Liu and Pan [25] discuss Big Data issues when many covariates are available. We can cite Fosen *et al.* [26], Zhao *et al.* [27], Giorgio *et al.* [28], Novák [29], Li *et al.* [30], where ABAO maintenances with static covariates are studied and estimation procedures are given and evaluated. Other designs were given by He *et al.* [31], Maitra *et al.* [32], Ning *et al.* [33] and Xu *et al.* [34]. Recurrent events data along with terminal event and covariates are discussed by Andersen *et al.* [35], Han *et al.* [36], Han *et al.* [37], Kim [38] and Sun *et al.* [39]. Frailty are sometimes also included such as in the work by Deep *et al.* [40], Lee *et al.* [41], Lin *et al.* [42] and Slimáček and Lindqvist [43]. In the four articles, an estimation method was provided. We can also cite Akacha and Ogundimu [44], who perform sensitivity analysis with missing recurrent event data influenced by covariates. However, none of these articles deal with imperfect maintenances. They all assume ABAO or AGAN repairs.

Very few articles work with models that include both covariates and imperfect maintenances. Wu and Scarf [45] consider the ARA models with dynamic covariates, but no estimation procedure is given. Peña [46] derives asymptotic properties of the estimator of the effect of the covariates without estimating the effect of the maintenances. Syamsundar and Naikan [47] estimate the effects of both covariates and maintenances. However, they only deal with two particular models and this procedure is not evaluated. Moreover, they only consider covariates that are constant between two failures. Claudio *et al.* [48] propose a maximum likelihood estimation with time-dependent covariates in the case of the Linear Extended Yule Process, which is an imperfect maintenance model different from the virtual age models. Li and Hanson [49] use Kijima's models along with step-wise constant covariates, but the covariates act on the maintenance effect, which will not be the case in this paper. Moreover, they use Bayesian inference. The generic model proposed by Doyen *et al.* [3] includes static covariates. They use the virtual age models in the same way as we do in this paper, providing methods for simulation and estimation. However, they do not study the statistical performance of the proposed model, and they only deal with constant covariates. Their framework was extended by Brenière *et al.* [50], who worked on virtual age models including both constant and time-dependent covariates, but without providing any in-depth nor thorough study of the quality of estimation. As an extended version of the work by Brenière *et al.* [50], the present article answers to this missing performance study: it develops a more detailed presentation of the proposed modeling framework and estimation methodology and, through numerical experiments, it investigates more in-depth the quality of estimation in the given mathematical framework. From an application point of view, this work contributes to a better understanding of the possibility to use virtual age models in presence of diverse and varying environments, represented by covariates; it considers thus closer-to-reality conditions and it can be considered as a step towards an enhanced applicability of these models, which is important for on-field application of advanced reliability modeling approaches.

1.2. Scope of this work

Here, we propose a way to include time-dependent covariates in a generic virtual age model. These covariates are linked to the failure process by an exponential factor in the conditional failure intensity. After recalling some useful definitions, in particular about

virtual age models, we set a mathematical framework. Each covariate is associated to a scalar, which intends to measure the influence of this covariate. The use of such an exponential factor is exposed by Cox [51]. Under this framework, we set up two simulation methods. The first one assumes that the covariates are step-wise constant to perform the exact inversion of the cumulative distribution function, while in the second one, the algorithm approximates the probability for the system to face a failure at each node of a fine time grid, to avoid an explicit inversion.

The other theoretical part of this paper deals with the estimation of the parameters of the model. These parameters are the ones of the baseline hazard rate (which characterizes the intrinsic wear of the systems), the scalar measuring the efficiency of the maintenances and the vector of the coefficients of the covariates influence. Our proposed estimation method works under the step-wise constant covariates assumption. It relies on the numerical maximization of the log-likelihood.

Finally, an extensive numerical study is conducted in order to assess the quality of estimation in the above-mentioned framework. In both the cases of constant covariates or time-dependent covariates, the focus is placed either on the influence of the parameters values, with large datasets, or on the influence of the data size, *i.e.* the number of systems in the dataset and the number of failures per system. We mainly use the Mean Squared Error (MSE) to analyse the quality of estimation of the model parameters.

Section 2 describes the theoretical framework, with first the mathematical writing of the model, then the description of the two simulation algorithms, and finally the estimation method. Section 3 is dedicated to the numerical study of the quality of estimation, with the constant and the time-dependent cases. We give a conclusion of this work and some future research prospects in Section 4.

2. Virtual Age Model With Covariates

2.1. Mathematical Framework

2.1.1. Definitions

Let us assume that we observe the n first failure times of a single repairable system $T_1, T_2, \ldots, T_n$, with $T_0 = 0$. Let $N = (N_t)_{t\geq 0}$ denote the counting process of failures. A stochastic model for this process of recurrent events is completely characterized by the intensity $\lambda = (\lambda_t)_{t\geq 0}$ of the failure counting process defined, for all $t \geq 0$, in Equation (1):

$$\lambda_t = \lim_{\Delta t \to 0} \frac{1}{\Delta t} \mathbb{P}(N_{t+\Delta t} - N_{t^-} = 1 | \mathcal{H}_{t^-}), \tag{1}$$

where $\mathcal{H}_{t^-}$ is the past of the process just before t and N_{t^-} represents the left-hand limit of N_t.

An imperfect maintenance model is composed of two parts. The first part of the model is the initial intensity, which corresponds to the hazard rate of the first time to failure and expresses the intrinsic wear of the new system before the first maintenance. Usually, the first failure time is assumed to follow a Weibull distribution, so that the initial intensity is

the intensity of a Power Law Process (PLP), $h(t) = \frac{\beta}{\eta}\left(\frac{t}{\eta}\right)^{\beta-1}$, for $t \geq 0$ and $\eta, \beta > 0$. β is a shape parameter while η is a scale parameter. The system is wearing for $\beta > 1$ and improving for $\beta < 1$. The second part of the model characterizes the maintenance effect on the system. The repair can be minimal, in which case the system is ABAO and the counting process is a Non Homogeneous Poisson Process of intensity $\lambda_t = h(t),\ t \geq 0$. The repair can also leave the system AGAN. The corresponding counting process is a Renewal Process of intensity $\lambda_t = h(t - T_{N_{t^-}}),\ t \geq 0$.

Between these two extreme cases, there is a wide range of models corresponding to imperfect maintenances. In this paper, we will focus on models that can be expressed in terms of virtual age, as defined by Doyen *et al.* [3] in Equation (2), for all $t \geq 0$:

$$\lambda_t = V'_{N_{t^-}}(t) h(V_{N_{t^-}}(t)). \tag{2}$$

After the ith failure, the system behaves like a new system which has not failed until $V_i(t)$, for $t \geq T_i$. This quantity is called the virtual or effective age of the system. Therefore, to define a model, we need to specify the initial failure intensity (also called baseline hazard rate) h and its parameters, and the virtual age after the ith failure, $V_i(t)$, which we make depend on an efficiency parameter ρ. With this generic model for the effect of the maintenances, we can consider ABAO maintenances with $V_i(t) = t$ and AGAN maintenances with $V_i(t) = t - T_i$.

2.1.2. Covariates

In order to take into account the observed heterogeneity between identical and independent systems, we introduce covariates in the virtual age model. The covariates are the recorded values of some indicators such as the geographic position of the system, which is a static information, or the temperature of the system while it is functioning, which can be measured continuously. Different systems exhibit different values of covariates, reflecting their heterogeneity. However, all the observed differences between the systems do not have the same influence on the failure process. This is why the covariates are associated to coefficients, that are constant over all the systems. A large (either positive or negative) coefficient indicates that the associated covariate has a great influence on the failure process. The sign of the coefficient tells us whether this influence is beneficial or harmful for the systems.

The covariates and their coefficients are included in the failure intensity via an exponential function like in the Cox's regression model [51]. Our generic model is written as in Equation (3), for all $t \geq 0$:

$$\lambda_t = V'_{N_{t^-}}(t) h(V_{N_{t^-}}(t)) \exp(\gamma' \mathbb{X}_t), \tag{3}$$

where $\mathbb{X}_t$ are the time-dependent covariates and γ are the coefficients associated to these covariates. If we only need static information, *i.e.* covariates that are constant with respect to time, we denote these static covariates $\mathbb{X}$.

2.1.3. Some particular virtual age models

The main models we will consider here are the ARA models, in the way they are defined by Doyen *et al.* [3]. In the ARA_∞ model developed by Doyen and Gaudoin [2], that

corresponds to the Type II Kijima's model [1] with deterministic constant maintenance effect, the repair is supposed to reduce the virtual age $V_{i-1}(T_i)$ by a factor $\rho \leq 1$, *i.e.* $V_{i-1}(T_i) - V_i(T_i) = \rho V_{i-1}(T_i)$. The corresponding virtual age is given in Equation (4), for all $0 \leq i \leq n$ and $t \geq T_i$:

$$V_i(t) = t - \rho \sum_{k=0}^{i-1} (1-\rho)^k T_{i-k}, \tag{4}$$

with the convention that the sum is null if $i = 0$. In the ARA_1 model developed by Doyen and Gaudoin [2], that corresponds to the Type I Kijima's model [1] with deterministic constant maintenance effect, the maintenance is supposed to reduce only the supplement of age since the last failure $V_{i-1}(T_i) - V_{i-1}(T_{i-1})$ by a factor $\rho \leq 1$, *i.e.* $V_{i-1}(T_i) - V_i(T_i) = \rho(V_{i-1}(T_i) - V_{i-1}(T_{i-1}))$. The corresponding virtual age is given in Equation (5), for all $0 \leq i \leq n$ and $t \geq T_i$:

$$V_i(t) = t - \rho T_i. \tag{5}$$

Between the ARA_1 and ARA_∞ models lie the ARA_m models, for $m \in \mathbb{N}^*$ (the memory of the model), with virtual age given in Equation (6), for all $0 \leq i \leq n$ and $t \geq T_i$:

$$V_i(t) = t - \rho \sum_{k=0}^{\text{Min}(m-1,i-1)} (1-\rho)^k T_{i-k}. \tag{6}$$

In all ARA models, the value of ρ represents the effect of repair. If $\rho \in]0,1[$ the repair is efficient, if $\rho = 1$ the repair is perfect (AGAN), if $\rho = 0$ the repair is minimal (ABAO) and if $\rho < 0$ the repair is harmful. In this paper, we will not consider harmful repairs so that $\rho \in [0,1]$.

Another usual imperfect maintenance model is the QR model, proposed by Wang and Pham [4], which considers that the times between two successive failures decrease or increase geometrically, depending on whether the system wears or rejuvenates. Under the QR model, the interfailure times verify the relation in Equation (7), for all $i \in \{1, \ldots, n\}$:

$$T_i - T_{i-1} = \rho^{i-1} Y_i, \tag{7}$$

where $(Y_i)_{i \in \{1,\ldots,n\}}$ is a sequence of independent identically distributed random variables with hazard rate $h(\cdot)$ and $\rho > 0$ is a parameter characterizing the effect of the repair. The corresponding counting process is also known as the geometric process as defined by Yeh [52] and its virtual age is given by (8), for all $0 \leq i \leq n$ and $t \geq T_i$:

$$V_i(t) = \frac{t - T_i}{\rho^i}. \tag{8}$$

The case $\rho = 1$ corresponds to the AGAN model. If $\rho \in]0,1[$, the system deteriorates due to stochastically decreasing interfailure times and if $\rho > 1$ the system improves. The last situation can occur when failed components of the system are replaced by new components built with new technologies.

2.2. Simulation of a dataset

We want to simulate failure times of systems with our model. A classical way to simulate realizations of a random variable is to compute the generalized inverse of its cumulative distribution function. Doyen *et al.* [3] simulate successive failure times by inverting the conditional cumulative distribution function, since the successive failure times of a system are not independent.

2.2.1. Simulation with constant covariates

Assuming the covariates $\mathbb{X}$ are constant, the conditional cumulative distribution function of T_{i+1} (the $(i+1)$th failure) knowing the past ($\mathcal{H}_{t^-}$) of the process and the covariates is given in Equation (9):

$$F_{i+1}(t) :=: F_{T_{i+1}|\mathcal{H}_{t^-},\mathbb{X}}(t) := \mathbb{P}(T_{i+1} \leq t|\mathcal{H}_{t^-}, \mathbb{X}) = 1 - \exp\left(-\int_{T_i}^{t} \lambda_s ds\right) \tag{9a}$$

$$= 1 - \exp\left(-\int_{T_i}^{t} V_i'(s) h(V_i(s)) \exp(\gamma' \mathbb{X}) ds\right) \tag{9b}$$

$$= 1 - \exp\left(-\exp(\gamma' \mathbb{X})(H(V_i(t)) - H(V_i(T_i)))\right), \tag{9c}$$

where $H(t) = \int_0^t h(s)ds$. Then we can compute the generalized inverse of F_{i+1}. Let U be a random uniform number between zero and one. We apply the generalized inverse of F_{i+1} on U in Equation (10):

$$T_{i+1} = \ F_{i+1}^{-1}(U) = V_i^{-1}(H^{-1}(H(V_i(T_i)) - \exp(-\gamma' \mathbb{X}) \log(1-U))), \tag{10}$$

where $V_i^{-1}(\cdot)$ is the generalized inverse of $V_i(\cdot)$ and $H^{-1}(\cdot)$ is the generalized inverse of $H(\cdot)$. We use this expression to simulate the successive failure times of a system.

2.2.2. Simulation with time-dependent covariates

When we consider time-dependent covariates, the expression of the cumulative distribution function is the same as in Equation (9a). Again, we would like to compute $F_{i+1}^{-1}(U)$ where $U \sim \mathcal{U}[0,1]$. In the general case, because of the $\exp(\gamma' \mathbb{X}_t)$ factor, which is time-dependent, in the intensity, we cannot explicitly invert the cumulative distribution function. Since F_{i+1} is non decreasing, we could use a simple incremental algorithm. To achieve this, we must be able to evaluate F_{i+1} in any point t. But when $\{\mathbb{X}_s\}_{s \geq 0}$ depends on the time, we cannot explicitely compute the integral. The integral could be computed numerically, but one integral has to be evaluated at each step of the inversion algorithm, which is too costly. To solve this issue, we propose two approaches.

First method. We make the following hypothesis: the covariates are piece-wise constant with respect to time, with a finite number L of constant steps. The discontinuity points of $\{\mathbb{X}_t\}_{t \geq 0}$ are deterministic and known. We note them τ_l, for all $0 \leq l \leq L-1$ (with $\tau_0 = 0$). The values taken by $\{\mathbb{X}_t\}_{t \geq 0}$ on the constant steps for a realization (system-dependent) are written $\chi_l,\ 1 \leq l \leq L$, with the mapping given in Equation (11):

$$\forall l \in \{1, \ldots, L-1\},\ \forall t \in [\tau_{l-1}, \tau_l[, \quad \mathbb{X}_t = \chi_l, \tag{11a}$$

$$\forall t \in [\tau_{L-1}, +\infty], \quad \mathbb{X}_t = \chi_L. \tag{11b}$$

Thus, with the convention $\tau_L = +\infty$, we can write Equation (12):

$$\mathbb{X}_t = \sum_{l=1}^{L} \chi_l \mathbf{1}_{[\tau_{l-1}, \tau_l[}(t). \tag{12}$$

It is important to notice that the $\{\chi_l\}_{1 \leq l \leq L}$ are random variables. The realization of χ_l is different for each system.

Thanks to our hypothesis, we can decompose the conditional cumulative distribution function as in Equation (13):

$$F_{i+1}(t) = 1 - \exp\left(- \sum_{l=1}^{L} \exp\left(\gamma' \chi_l\right) \int_{\max(T_i, \tau_{l-1})}^{\min(t, \tau_l)} V_i'(s) h(V_i(s)) ds \right). \tag{13}$$

The computation of $F_{i+1}(t)$ depends on the discontinuity points τ_{l-1} and τ_l between which T_i and t lie. Between two discontinuity points, the covariates are constant and their value can be taken out of the integral so that the integrand no longer depends on l. We then introduce this notation: $l_{(t)} \in \{1, \ldots, L\}$ is such that $t \in [\tau_{l_{(t)}-1}, \tau_{l_{(t)}}[$, *i.e.* $l_{(t)} = \sum_{l=0}^{L-1} \mathbf{1}_{\{\tau_l \leq t\}}$ is the cumulative number of covariate steps at time t. After some computations, which are detailed in Appendix A, we can write Equation (14):
if $l_{(T_i)} = l_{(t)}$,

$$F_{i+1}(t) = 1 - \exp\Big(- \exp(\gamma' \chi_{l_{(T_i)}}) \left(H(V_i(t)) - H(V_i(T_i)) \right) \Big); \tag{14a}$$

else,

$$\begin{aligned} F_{i+1}(t) = 1 - \exp\Bigg(& - \sum_{l=l_{(T_i)}+1}^{l_{(t)}-1} \exp(\gamma' \chi_l) \left(H(V_i(\tau_l)) - H(V_i(\tau_{l-1})) \right) \\ & - \exp(\gamma' \chi_{l_{(T_i)}}) \Big(H(V_i(\tau_{l_{(T_i)}})) - H(V_i(T_i)) \Big) - \exp(\gamma' \chi_{l_{(t)}}) \Big(H(V_i(t)) - H(V_i(\tau_{l_{(t)}-1})) \Big) \Bigg), \end{aligned} \tag{14b}$$

the sum being eventually empty if $l_{(T_i)} = l_{(t)} - 1$.

Then we perform the exact inversion of the conditional cumulative distribution function. A random uniform number U between zero and one is drawn. After having computed the number of the covariate step where the last failure time lies ($l_{(T_i)}$), we take it as a starting point for the search for the covariate step where the next failure will occur. This step corresponds to $l_{(t)}$. To achieve this, since $F_{T_{i+1}}$ is non-decreasing, we iteratively compute its value at each discontinuity point of the covariates τ_l, $l_{(T_i)} \leq l \leq L - 1$. When this value exceeds U for the first time, at the point denoted $\tau_{l_{(t)}}$, we know that the next failure time will occur within the covariate step $l_{(t)}$. Then we can explicitly compute $F^{-1}_{T_{i+1}}(U)$ as in

Equation (15):
if $l_{(T_i)} = l_{(t)}$,

$$F_{T_{i+1}}^{-1}(U) = V_i^{-1}\left(H^{-1}\left(H(V_i(T_i)) - \exp(-\gamma'\chi_{l_{(T_i)}})\log(1-U)\right)\right); \tag{15a}$$

else,

$$F_{T_{i+1}}^{-1}(U) = V_i^{-1}\left(H^{-1}\left(H(V_i(\tau_{l_{(t)}-1})) - \exp(-\gamma'\chi_{l_{(t)}}) \times (S + \log(1-U))\right)\right), \tag{15b}$$

where

$$S = \sum_{l=l_{(T_i)}+1}^{l_{(t)}-1} \exp(\gamma'\chi_l)\Big(H(V_i(\tau_l)) - H(V_i(\tau_{l-1}))\Big) + \exp(\gamma'\chi_{l_{(T_i)}})\Big(H(V_i(\tau_{l_{(T_i)}})) - H(V_i(T_i))\Big). \tag{15c}$$

Second method. In case we can record the values of the covariates continuously, we can use the previous simulation method with a discretization of these covariates. We propose another method for failure times simulation in which there is no need to perform the inversion of the conditional cumulative distribution function. We postulate that we know the values of the covariates at each time of the form $k\Delta t,\ k \in \mathbb{N}^*$. Then we suppose that the possible time of the next failure is also of the form $k\Delta t,\ k \in \mathbb{N}^*$. If we assume that the failure intensity is constant on a short time interval of length Δt, we can approximate the probability of the next failure time to be Δt later with Equation (16):

$$\mathbb{P}(T_{i+1} \leq T_i + k\Delta t | \mathcal{H}_{T_i}, T_{i+1} > T_i + (k-1)\Delta t) = 1 - e^{-\int_{T_i+(k-1)\Delta t}^{T_i+k\Delta t} \lambda_s ds} \simeq 1 - e^{-\lambda_{T_i+k\Delta t}\Delta t}. \tag{16}$$

To know whether a failure occurs in $T_i + k\Delta t$, we draw a random variable with a Bernoulli distribution of parameter $1 - e^{-\lambda_{T_i+k\Delta t}\Delta t}$. With this simplification, we can set up an algorithm for the simulation of the next failure time, which is displayed in Listing 1.

Listing 1: Alternative simulation algorithm

```
initialization: k=0, D=0;
while (D==0) do:
   k ← k+1;
   λ(k) ← λ_{T_i+k*Δt};
   D ← draw of a random variable with a Bernoulli
         distribution of parameter 1-exp(-λ(k)*Δt);
end while;
T_{i+1} ← T_i + k*Δt;
output: T_{i+1};
```

nb. of failures	scale of PLP	shape of PLP	efficiency of maint.	coef. of covariate
$n = 15$	$\eta = 0.5^{-1/3}$	$\beta = 3$	$\rho = 0.35$	$\gamma = 0.3$

Table 1: Parameters of the simulated dataset given in example

2.2.3. Example of a simulated dataset

In order to illustrate the simulation algorithm with the influence of covariates, a simulated dataset is shown here. We simulated three systems of failure times influenced by a covariate, with the first method exposed in 2.2.2. They all have been simulated with the ARA_∞ model and with the same parameters, that are displayed in Table 1. Only the values of the covariate change with the system. The covariate is a jump process that jumps at times $\{2, 3, 4, 6, 8\}$. Each jump is a realization of a random variable with Gamma distribution with rate 1 and scale α, where α is the length of the step multiplied by 1, 2 or 4 respectively for the three systems. For the first system, the covariate grows slowly. For the third one, the covariate increases quickly. The second system lies in between. In Figure 1, the values of the covariate are represented versus time, for each system. In Figure 2, we see the corresponding simulated failure times. The counting process is represented versus time.

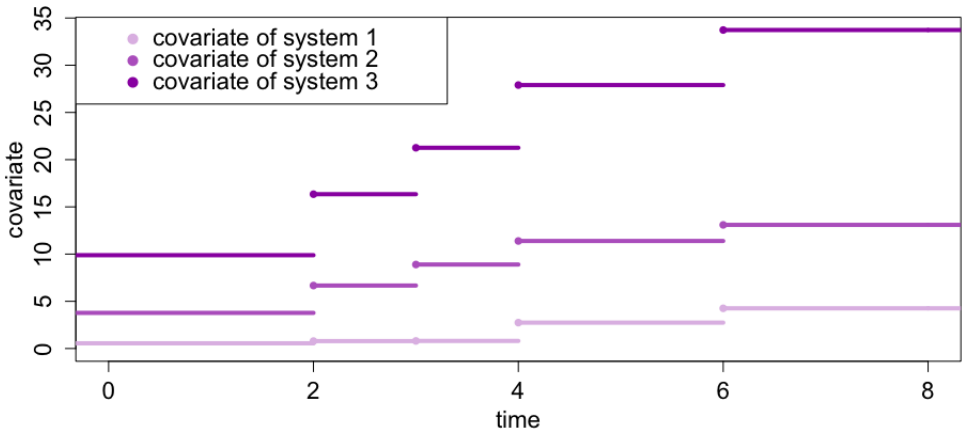

Figure 1: Example of three covariate paths considered for failure times simulation

We can clearly see the influence of the covariate on the failure process. The main goal now is to extract information from data both about the maintenance model and about the covariate influence.

2.2.4. Comparison of the two simulation methods

We compared the two methods exposed in this subsection. In what follows, we refer as "the first method" to the one where the exact inversion of the cumulative distribution function is performed, and as "the second method" to the one where the failure probability is approximated at each covariate step.

We compared the simulation speed of the two methods. We found that with a covariate that jumps with a high frequency, the second method is about 3.5 times faster than the first

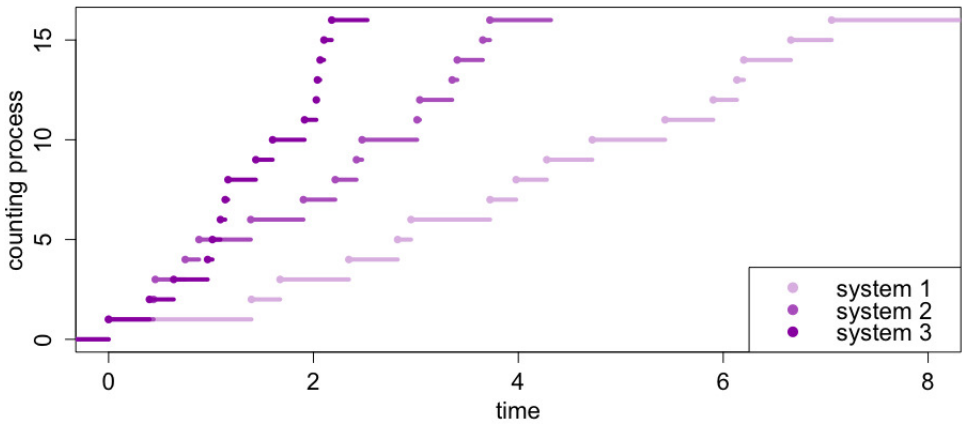

Figure 2: Counting process of the failures for the three considered covariate paths

one. Conversely, if we have a covariate with a low jump frequency, it is two times faster to use the first method with one value per jump than the second method with a covariate constant for some steps. It is not recommanded to use the second method with large covariate steps since it would not be accurate in this case.

2.3. Estimation of the model parameters

The estimation of the parameters of the virtual age model with covariates is done by maximizing numerically the log-likelihood of the model with the given data.

2.3.1. Method

We write here the computations for a single system, the total log-likelihood being merely the sum of the log-likelihood of each system, keeping in mind that the values of the covariates and of the virtual age depend on the system. We observe the system either until a fixed time $\mathcal{T}$ or until it reaches a fixed amount of n failures, *i.e.* $\mathcal{T} = T_n$. With $T_{N_{\mathcal{T}^-}+1} = \mathcal{T}$, the log-likelihood can be written as in Equation (17):

$$\mathcal{L} = \sum_{i=1}^{N_{\mathcal{T}}} (\log(\lambda_{T_i})) - \int_0^{T_{N_{\mathcal{T}^-}+1}} \lambda_s ds. \tag{17}$$

The issue is fundamentally the same as in the simulation: the value of the covariates depends on the time.

Computation of the log-likelihood. The computation of the sum, given in Equation (18), is rather simple if we find $l_{(T_i)} \in \{1, \dots, L\}$ for $1 \leq i \leq N_{\mathcal{T}}$ such that $T_i \in [\tau_{l_{(T_i)}-1}, \tau_{l_{(T_i)}}[$:

$$\sum_{i=1}^{N_{\mathcal{T}}} (\log(\lambda_{T_i})) = \sum_{i=1}^{N_{\mathcal{T}}} \log(V'_{i-1}(T_i)) + \sum_{i=1}^{N_{\mathcal{T}}} \log(h(V_{i-1}(T_i))) + \sum_{i=1}^{N_{\mathcal{T}}} \gamma' \chi_{l_{(T_i)}}. \tag{18}$$

In order to compute the integral, we set a partition of the time composed by the failure times and the discontinuity points of the covariates. Indeed, each time there is a new failure,

the value of the virtual age changes and each time we reach a discontinuity point, the values of the covariates change. Since these two quantities are involved in the computation of the failure intensity λ_s, we need to trace these modifications. First, we gather all the change points in a single ordered vector $\varsigma = (\varsigma_k)_{k\in\{0,\dots,N_{\mathcal{T}^-}+L\}}$. We introduce two counters: $\ell_k = \sum_{l=0}^{L} \mathbf{1}_{\{\tau_l \le \varsigma_k\}}$, which is the number of the current covariate step, and $\imath_k = \sum_{i=1}^{N_{\mathcal{T}^-}+1} \mathbf{1}_{\{T_i \le \varsigma_k\}}$ which is the current number of failures, where $k \in \{0, \dots, N_{\mathcal{T}^-} + L\}$ is the number of the segment in the partition. A graphical example is given in Figure 3, displaying the values of k, ℓ_k and $\imath_k$ on some segments, where ς_k is the lower bound of the kth segment.

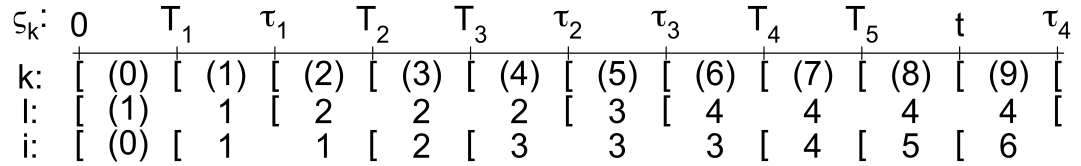

Figure 3: Here is an example of the way failure times and discontinuity points of covariates can lie. On this graph, they are evenly placed, while in fact it is not necessarily the case.

We always have $\varsigma_0 = 0$ (time begins at zero), $\ell_0 = 1$ (it is the first step of the covariates) and $\imath_0 = 0$ (no failure occurred before the end of the first segment). Then the integral is the sum of the integrals restricted to each segment, until we reach $T_{N_{\mathcal{T}^-}+1}$, as in Equation (19):

$$\int_0^{T_{N_{\mathcal{T}^-}+1}} \lambda_s ds = \sum_{k=0}^{K} \exp(\gamma' \chi_{\ell_k}) \left(H(V_{\imath_k}(\varsigma_{k+1})) - H(V_{\imath_k}(\varsigma_k)) \right), \tag{19}$$

where $K \in \{0, \dots, N_{\mathcal{T}^-} + L\}$ is such that $\varsigma_{K+1} = T_{N_{\mathcal{T}^-}+1}$.

Equations (18) and (19) provide a general computable expression for the log-likelihood.

Maximization of the log-likelihood. The way of optimizing the log-likelihood is taken from Doyen *et al.* [3]. We assume that the baseline hazard rate is a function of time with two parameters: β, a shape parameter; and α, a scale-like parameter that is a factor in the baseline hazard rate. For example, the Weibull distribution can be rewritten as in Equation (20), with $\alpha = 1/\eta^\beta$, where η is the true scale parameter of the Weibull distribution:

$$h(t) = \frac{\beta}{\eta} \left(\frac{t}{\eta} \right)^{\beta-1} = \alpha\beta t^{b-1}. \tag{20}$$

We denote $\tilde{h}(t) := h(t)/\alpha,\ t \le 0$. Therefore, the model parameters to estimate are α, β, ρ and γ. Then, from Equations (18) and (19), we get Equation (21):

$$\mathcal{L} = N_{\mathcal{T}} \log \alpha - \alpha S_1(\beta, \rho, \gamma) + S_2(\beta, \rho) + S_3(\rho) + S_4(\gamma), \text{ where} \tag{21a}$$

$$S_1(\beta,\rho,\gamma) := \sum_{k=0}^{K} \exp(\gamma'\chi_{\ell_k}) \left(\tilde{H}(V_{\imath_k}(\varsigma_{k+1})) - \tilde{H}(V_{\imath_k}(\varsigma_k)) \right), \tag{21b}$$

$$S_2(\beta,\rho) := \sum_{i=1}^{N_{\mathcal{T}}} \log(\tilde{h}(V_{i-1}(T_i))), \tag{21c}$$

$$S_3(\rho) := \sum_{i=1}^{N_{\mathcal{T}}} \log(V'_{i-1}(T_i)) \text{ and} \tag{21d}$$

$$S_4(\gamma) := \sum_{i=1}^{N_{\mathcal{T}}} \gamma'\chi_{l_{(T_i)}}. \tag{21e}$$

The unique value of α maximizing the log-likelihood is equal to $N_{\mathcal{T}}/S_1(\beta,\rho,\gamma)$. Therefore, the optimization can be performed only over β, ρ and γ with the formula given in Equation (22):

$$(\hat{\beta},\hat{\rho},\hat{\gamma}) = \underset{\beta,\rho,\gamma}{\operatorname{argmax}}\, L(\beta,\rho,\gamma), \text{ where} \tag{22a}$$

$$L(\beta,\rho,\gamma) = N_{\mathcal{T}}(\log N_{\mathcal{T}} - \log S_1(\beta,\rho,\gamma)) - N_{\mathcal{T}} + S_2(\beta,\rho) + S_3(\rho) + S_4(\gamma) \text{ and} \tag{22b}$$

$$\hat{\alpha} = N_{\mathcal{T}}/S_1(\hat{\beta},\hat{\rho},\hat{\gamma}). \tag{22c}$$

2.3.2. Example of parameters estimation

In subsection 2.2, we have simulated a dataset of failure times, with $\nu = 3$ systems facing $n = 15$ failures each, with the first method exposed in 2.2.2. The underlying model is the ARA_∞-PLP model with one covariate. We recall its failure intensity in Equation (23), keeping in mind that each system is linked to different values of the covariate:

$$\lambda_t = \frac{\beta}{\eta} \left(\frac{1}{\eta} \left(t - \rho \sum_{k=0}^{N_{t^-}-1} (1-\rho)^k T_{N_{t^-}-k} \right) \right)^{\beta-1} \exp(\gamma'\mathbb{X}_t). \tag{23}$$

These systems are under the influence of an increasing step-wise constant covariate.

In Figure 4, in the left part, we have represented the contour of the log-likelihood of the ARA_∞-PLP model for this dataset with respect to the coefficient of the covariate and ρ, while β is supposed to be known. In the right part, we have represented the same log-likelihood but with respect to β and ρ, while the coefficient of the covariate is supposed to be known. On both plots, we can clearly see a maximum point. This is the point we are looking for: the maximum likelihood estimation of the parameters.

For the same simulated dataset, we have numerically maximized the log-likelihood of the ARA_∞-PLP model. We can either perform a partial estimation, which matches Figure 4, or a total estimation of all the parameters. We find the estimates given in Table 2. These estimations are quite satisfying, especially if we recall that the dataset is not very large (only three systems) and that we have four parameters to estimate.

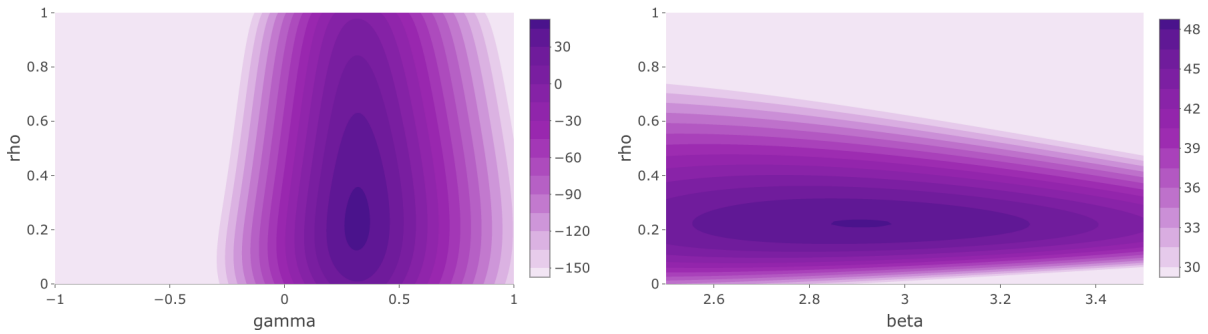

Figure 4: Example of log-likelihood contour versus the values of the coefficients of the covariate and efficiency (left) and versus the values of the parameters of the virtual age model (right)

		η	β	ρ	γ
simulation values		1.26	3	0.35	0.3
estimated values when{	β known	1.66	/	0.22	0.32
	γ known	1.58	2.91	0.22	/
	all unknown	1.88	3.42	0.23	0.36

Table 2: Simulation values, partial estimations and total estimations of the four parameters of the model

3. Quality of estimation of the model parameters: comprehensive numerical study

The aim in this section is to evaluate the statistical performance of the estimation method exposed in Subsection 2.3. To achieve this, a numerical study has been set up. It consists in simulating a large number of datasets with a virtual age model and fixed parameters, which was done here with the first method exposed in 2.2.2 and, from the obtained datasets, estimating the parameters of the model as if the true parameters were not known. The numerical maximization of the log-likelihood was performed with the Nelder-Mead method [53], that does not require to compute the gradient of the objective function. The initial values were $\beta = 2.1$, $\rho = 0.55$ for the ARA models, $\rho = 0.82$ for the QR model and $\gamma = 0$. The result is a collection of estimations, which have to be compared to the true values used for the simulation. A common statistic for the evaluation of the quality of estimation is the Mean Squared Error (MSE), which balances the bias of the estimations with their standard deviation. The empirical formula of the MSE for a set $\hat{\theta}_{(M)} := (\hat{\theta}_m)_{1 \leq m \leq M}$ of M estimations of a parameter θ_0 is given in Equation (24):

$$MSE(\hat{\theta}_{(M)}) = s^2_{\hat{\theta}_{(M)}} + (m_{\hat{\theta}_{(M)}} - \theta_0)^2, \tag{24}$$

where $m_{\hat{\theta}_{(M)}}$ is the empirical mean of $\hat{\theta}_{(M)}$, $s^2_{\hat{\theta}_{(M)}}$ is its empirical variance and θ_0 is the true parameter used for simulation. The parameter η_0 is a scale parameter. In the time-dependent covariate case, we fixed its value in the simulations so that all the 20 failures of each system occurred approximately within the same range of time, which consists in the range of the

jump times of the covariate. To achieve this, we simulated a dataset with several systems and we computed the mean of the $20th$ failure times of the systems. It corresponds to the empirical expectation of the $20th$ failure time. This mean was expected to lie around the time of the last covariate jump. We repeated this procedure while changing the value of η_0 until the mean fell approximately on the last jump time of the covariate. Therefore, the values taken by this parameter are very heterogeneous and depend on the considered model and on the value of the other parameters. For example, in the situation of Section 3.2.1, we have $\eta_0 = 0.02$ for the ARA_1 with $\beta_0 = 1.5$ and $\rho_0 = 0.1$, and $\eta_0 = 0.0006$ when $\beta_0 = 3$ and $\rho_0 = 0.1$. In order to analyse the quality of estimation without being biased by the true value η_0, all the MSE of this parameter have been normalized. The normalized MSE are denoted nMSE and are computed as in Equation (25):

$$nMSE(\hat{\theta}_{(M)}) = \frac{1}{\theta_0^2} MSE(\hat{\theta}_{(M)}). \tag{25}$$

The study focuses on the ARA_1, ARA_∞ and QR models, with a PLP initial intensity of scale parameter η_0 and shape parameter β_0. However, in most cases, the results with the two ARA models are quite similar. Therefore, the graphs do not display the two models, but only the ARA_∞ model. The model includes a unidimensional covariate which is simulated either as a uniform random variable (constant covariate), as a cumulated sum of such variables (time-dependent covariate), or as a random variable that takes its values in a finite state space.

In all graphs of this section, μ is a shortcut for 10^{-6}.

3.1. Constant covariate

In this subsection, we work with a constant covariate. The first part of the study is devoted to the influence of the shape parameter β of the Weibull distribution, the efficiency parameter ρ of the virtual age model and the coefficient of influence γ of the covariate on the quality of estimation. For each configuration, $M = 10000$ datasets have been simulated, with a fixed number of systems per dataset and a fixed number of failures per system, and then used in estimation. In order to focus on the influence of the model parameters on the quality of estimation, this part is done with large datasets with fixed size: the number of systems per dataset is fixed to $\nu = 50$ and the number of failures per system to $n = 20$. With such datasets, it is expected to get results that are not polluted by a too small data size. The second part of the study is devoted to the influence of the data size. The parameters of the model are fixed but the number of systems per dataset and of failures per system varies.

3.1.1. Influence of the parameters of the virtual age model and of the baseline hazard rate

Settings. A time-constant covariate was simulated as a uniform random variable between 0 and 1 for each system. The true coefficient of influence of this covariate was set to $\gamma_0 = 1$. The Weibull scale parameter was set to $\eta_0 = 1/(0.1^{1/\beta_0})$. Its shape parameter β_0 varied in the set $\{1.5, 1.75, \ldots, 3\}$ and the efficiency parameter ρ_0 varied in the set $\{0.1, 0.2, \ldots, 0.9\}$ in case of an ARA model, and in $\{0.7, 0.75, \ldots, 0.95\}$ in case of the QR model. We recall that, in the virtual age model, the higher ρ_0 is, the more efficient the maintenance is. In

particular, when $\rho_0 = 1$, the process described by the ARA models and the QR model is a Renewal Process, which means the system is left AGAN after each maintenance. However, in the case of the QR model, if ρ_0 is too far from 1, the failures occur within a very short time range. This is easily understandable when looking at Equation (7), which gives the distribution of the interfailure times: stochastically, they exponentially decrease. Moreover, in the baseline hazard rate, the higher β is, the faster the system is wearing.

Heatmaps. Heatmaps of the empirical MSE obtained in this setting are given in Figure 5. These MSE are computed for each of the four estimated parameters: β and η, respectively the shape and scale parameters of the Weibull distribution, are on the upper part. γ, the coefficient of the covariate, is on the lower left, while ρ, the efficiency of the maintenances, is on the lower right. In each of these quadrants, there are two heatmaps: the one on the left is for the ARA_∞ model, the other one is for the QR model. As stated in the beginning of this section, the ARA_1 model is not displayed in the heatmaps, since it exhibits patterns that are very similar to the ones of the ARA_∞ model.

General results. The first thing to notice on Figure 5 is that the results seem very satisfying: all the values of the MSE are reasonably low, and so are the biases: no more than 0.018 for β, 0.06 for ρ and 0.011 for γ, and the standard deviations: no more than 5 % of the true value for β, 9 % for η, 12 % for γ. The standard deviations of ρ highly depend on its true value and on the value of β_0 in the case of the ARA models (it is no more than 0.4 % for the QR model): the higher ρ_0 and β_0 are, the lower the relative standard deviation is. We did the same study without any covariate in order to have reference values. It turned out that for β, η and ρ, the MSE are very similar when looking at the pattern of the heatmaps and that for the parameter η, the MSE are generally a bit higher in the case of the QR model, but almost the same with the ARA models, and with all models for β and ρ. This means that the simultaneous estimation of the effect of a covariate does not affect significantly the estimation of the parameters of the baseline hazard rate and of the virtual age model.

Influence of the parameters. Finally, we can analyse the variations of the MSE versus the true values β_0 and ρ_0: within the ARA_∞ model, β is better estimated when ρ_0 is high, and also slightly better estimated when its own true value is low. This may be due in most configurations to the mere scale of the parameter, and in fact we observe for example that the MSE for $\beta_0 = 1.5$ are higher than one fourth of the ones for $\beta_0 = 3$. Within the QR model, the higher ρ_0 is and the lower β_0 is, the better the estimations are.

The shape parameter of the Weibull distribution β_0 has a clear influence on the quality of estimation of the scale parameter of this distribution within the ARA models: the nMSE of the estimations of η are far lower when β_0 is high. ρ_0 does not have such an obvious influence, but it looks like high values of this parameter are correlated with slightly better estimations of η. Within the QR model, there is also a slight improvement of the estimations when β_0 is high, but above all, the higher ρ_0 is, the better the estimations are. We already pointed out the fact that if ρ_0 is too far from 1 within the QR model, the interfailure times are very small, making the estimation of the parameters more difficult.

The true values of β and ρ have almost no influence on the quality of estimation of γ. The MSE may be slightly lower within the ARA models when ρ_0 is high, but the difference is not very big: from 0.0137 to 0.0158.

Regarding the quality of estimation of ρ, we can say that the higher β_0 is, the better the estimation of ρ is, regardless of the model (except for $\rho_0 = 0.7$ within the QR model). The true value ρ_0 also impacts its quality of estimation within all models. Higher true values are preferable in the QR model. It is the reverse with the ARA_∞ model for $\rho_0 \leq 0.7$. For lower values, the quality of estimation is again slightly better.

For β, η and ρ, we find that within the ARA models, the standard deviation weights more than the bias in the value of the MSE, whereas the weights are more or less the same within the QR model.

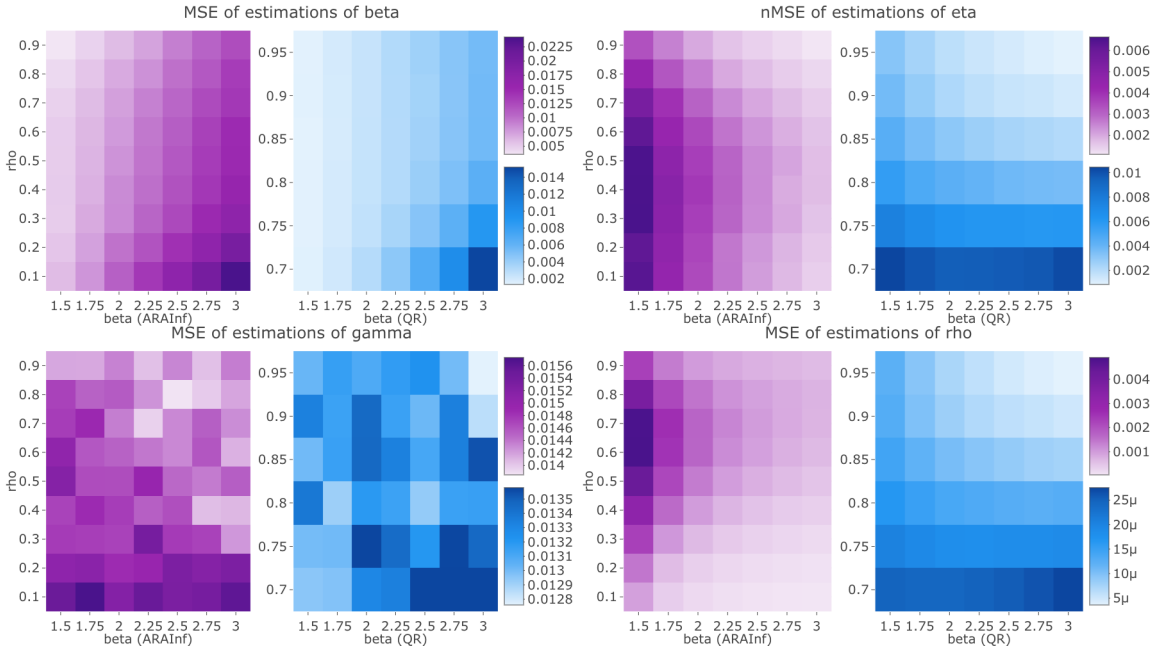

Figure 5: MSE of the estimations of the four parameters in the case of a constant covariate, versus the true values of β_0 and ρ_0

3.1.2. Influence of the coefficient of the covariate

We focus here on the influence of γ_0 on the quality of estimation. This time, only the case $\eta_0 = 1/(0.1^{1/2.5})$, $\beta_0 = 2.5$, $\rho_0 = 0.7$ for the ARA models and $\rho_0 = 0.9$ for the QR model was considered while γ_0 varied in the set $\{-3, -2, \ldots, 3\}$. Plots of the empirical MSE obtained in this setting are given in Figure 6. We see again that the results are satisfyingly good, with even better results in the case of the QR model. We find no significant influence of the true value γ_0 on the quality of estimation of the three other parameters. Moreover, the biases are very low for all parameters (at most 0.016 for β, 0.060 for η, 0.0018 for γ and 0.0020 for ρ), as well as the standard deviation for β, η and ρ (at most 0.010 for β, 0.018 for η, 0.17 for γ and 0.032 for ρ), with respect to the true values of the parameters.

The plot for γ in Figure 6 is very intriguing: its symmetrical look tells us that the influence of the covariate weights equally whether γ_0 is positive or negative. The more the absolute value of γ_0 increases, the higher the MSE is. The curves have a quadratic look, but we cannot directly infer such a conclusion. However, we have to recall that the MSE is composed of the squared bias and of the variance. Therefore, its value has the order of magnitude of the squared true value of the parameter. The variation of the MSE in function of the true value γ_0 could be mathematically studied in future works. We point out that this variation comes mostly from the standard deviation, since the biases of γ are 10 to 600 times lower than the standard deviations. Within the ARA models, the biases show a very slight trend to underestimate (in absolute value) γ. Nevertheless, these biases are very low, always under 0.02, for a true value of $\gamma_0 = 1$.

The plot for γ in Figure 6 also exhibits an interesting feature: the three curves, corresponding to the three studied models, meet in a single point at $\gamma_0 = 0$. This may also be a mathematical property worth being studied, as well as the fact that the quality of estimation of the other parameters is not impacted by the value γ_0.

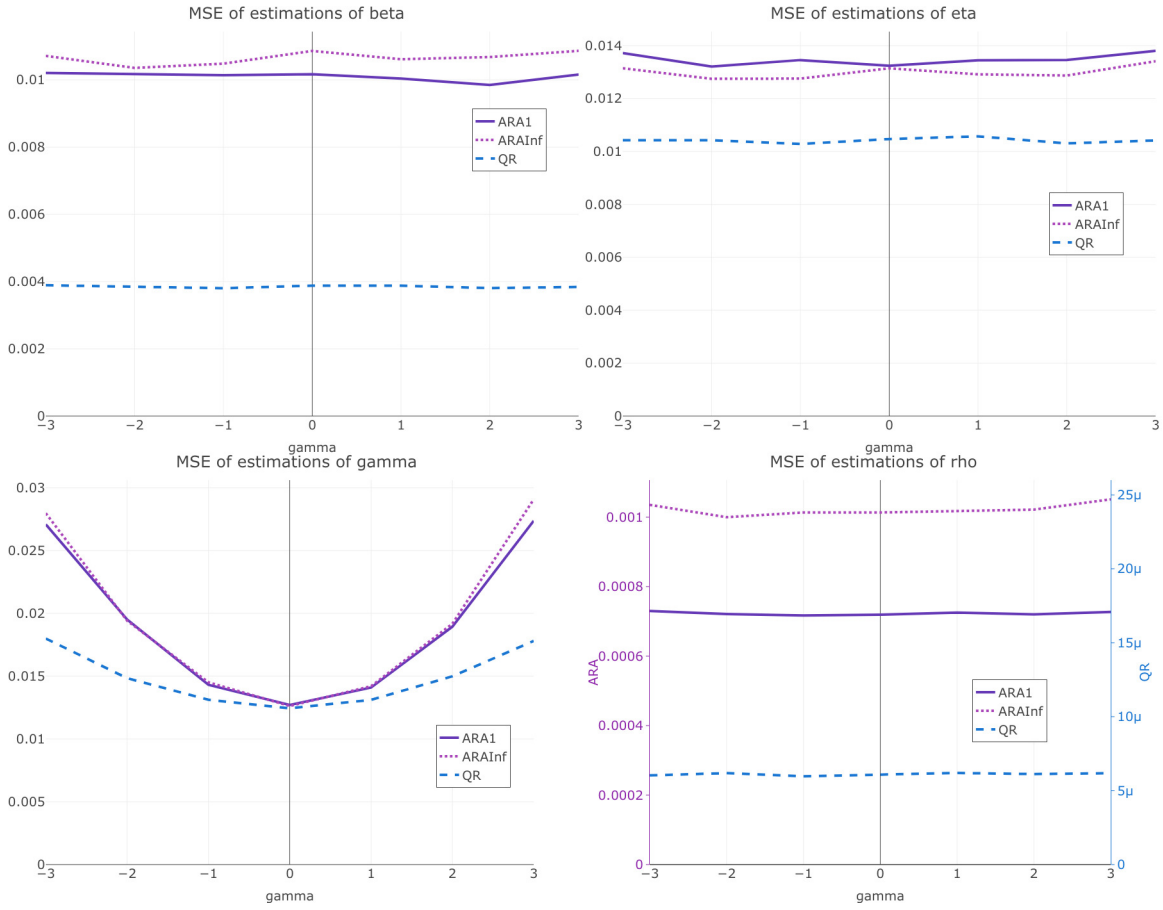

Figure 6: MSE of the estimations of the four parameters in the case of a constant covariate, versus the true values of γ_0

3.1.3. Influence of data size on the quality of estimation

Settings. This part of the numerical study intends to analyse how the dimensions of the datasets influence the quality of estimation. The dimensions of a dataset are the number of identical and independent systems that are observed, which is denoted ν, and the number of failures that each system faces. Here, we chose to observe each system (*i.e.* to run the simulation) until a fixed number of n failures happened. Other possibilities can be encountered: each system can be observed until reaching its own fixed number of failures, or until the end of a fixed observation time.

We allowed these two parameters to vary in the set $\{5, 10, 15, \ldots, 50\}$. With this choice, we were able to compare the performances with a fixed number of systems and a varying number of failures, and *vice versa*, or with a fixed total number of failures. For example, 10×10 (10 systems with 10 failures each), 5×20, or 20×5 datasets all correspond to a total number of failures of 100. In order to focus on the data size, we chose the model parameters among ones that showed good results: $\rho_0 = 0.7$ for the ARA models, $\rho_0 = 0.9$ for the QR model, $\eta_0 = 1/(0.1^{1/2.5})$, $\beta_0 = 2.5$, $\gamma_0 = 1$. The constant covariate was simulated as previously as a uniform random variable between 0 and 1. For each pair of ν and n, we simulated $M = 10000$ datasets.

Heatmaps. Heatmaps of the empirical MSE obtained in this setting are given in Figure 7. These MSE are computed for each of the four estimated parameters: β and η are on the upper part. γ is on the lower left, while ρ is on the lower right. In each of these quadrants, there are two heatmaps: the one on the left is for the ARA_∞ model, the other one is for the QR model. Each heatmap displays the MSE versus n, the number of failures per system, on the horizontal axis, and ν, the number of systems, on the vertical axis. The look of Figure 7 is immediately satisfying: we see a clear trend to get better estimations when the data size increases, either in terms of number of systems or of number of failures.

Parameters of the Weibull distribution. For β, we observe a symmetrical heatmap with the QR model, but with the ARA_∞ model, this is not the case. We find it is easier to estimate β with more systems than with more failures per system. For example, the MSE of β with datasets of 5 systems and 15 failures is approximately 0.20, whereas with datasets of 15 systems and 5 failures, the MSE is approximately 0.12, *i.e.* only about 60 % of the former. A natural explanation for this is that β is the shape parameter of the baseline hazard rate, which corresponds to the failure intensity of the first failure time of a system. Therefore, we have more information about β when we have several systems. We observe the same thing for η, which is the scale parameter of the baseline hazard rate, and it is visible even with the QR model.

Efficiency of the maintenances. It is interesting to see the reverse is true for ρ within the QR model: since ρ corresponds to the maintenance efficiency, it is coherent that its estimations are better with more failures per system. Quite surprisingly, it does not happen with the ARA_∞ model. As a possible explanation, we may say that the better estimations of ρ with the ARA_∞ model when there are more systems are linked to the better estimations of β an η that happen in this case. Indeed, β and ρ compensate for each other in the virtual age model:

a system which wears slowly (*i.e.* with a low β) with poorly efficient maintenances (*i.e.* a low ρ) may exhibit a realization of the failure process similar to the one we could get with a system that wears quickly (high β) with more efficient maintenances (high ρ). Therefore, if for example β is overestimated for a dataset, it may be linked to an overestimation of ρ for the same dataset. This would explain why we have better estimations of ρ with the ARA_∞ model when there are several systems. The QR model does not show the same trend, but we can postulate that this is due to a distinctive feature of this model: the interfailure times are distributed as independent and identically distributed random variables multiplied by the successive powers of ρ. Consequently, it is easy to estimate ρ with a small number of failures per system: we see that we have very good results starting from only 10 failures per system, whatever the number of systems is.

Coefficient of the covariate. Regarding γ, we find that the estimations are far from being as good as with large datasets. We see that the results are better when there are more systems than when there are more failures per system. Within the ARA_∞ model for example, with 5 systems facing 25 failures each, the MSE of γ is about 0.13, whereas with 25 facing 5 failures each, the MSE is about 0.06, *i.e.* less than a half of the former. This is also true with the QR model. A way to explain this is to consider the size of data useful for the estimation of γ. With only one system, it is impossible to estimate γ, since it is undistinguishable from the scale parameter η. The need of the covariate comes from the presence of several identical and independent systems. Each system corresponds to a single value of the covariate. With one constant covariate as it is the case here, we only have one data point per system, whichever the number of failures is. In the previous example, in order to estimate γ, we only have 5 data points in the former case, and 25 in the latter. In comparison, the estimation of η and β relies on all the $25 \times 5 = 125$ data points, and on $24 \times 5 = 120$ or $25 \times 4 = 100$ data points for ρ (the first failure time carries no information on ρ, since there has been no maintenance yet).

For all parameters, the standard deviation weights more in the value of the MSE than the bias. The biases are in all cases very satisfying, but can we observe an interesting phenomenon for the parameters η and ρ. Within the ARA models, the biases are lower when there are more systems whereas within the QR models, the biases are lower when there are more failures per system.

3.2. Time-dependent covariate

3.2.1. Influence of the parameters of the virtual age model and of the baseline hazard rate

Settings. In this subsection, we analyse the influence of the shape parameter β_0 of the Weibull distribution and of the efficiency parameter ρ_0 of the virtual age model. Likewise in Subsection 3.1, $M = 10000$ datasets have been simulated for each configuration, with $\nu = 50$ systems per dataset and $n = 20$ failures per system. The ranges of values of the parameters were the same: the true coefficient of influence of the covariate was set to $\gamma_0 = 1$, β_0 varied in the set $\{1.5, 1.75, \ldots, 3\}$ and ρ_0 varied in the set $\{0.1, 0.2, \ldots, 0.9\}$ in case of an ARA model, and in $\{0.7, 0.75, \ldots, 0.95\}$ in case of the QR model. η_0 was chosen so that all the failures occurred within a comparable range of time. The difference lies in the

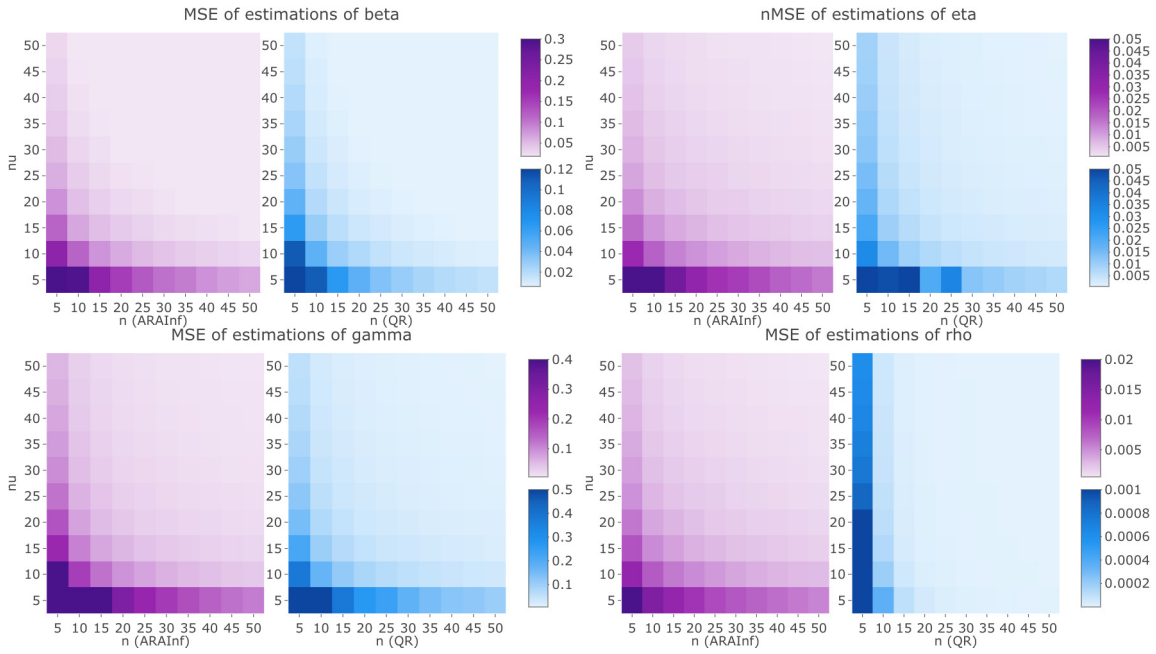

Figure 7: MSE of the estimations of the four parameters in the case of a constant covariate, versus the number n of failures per system and the number ν of systems per dataset

type of the covariate: here, it was no longer a constant covariate, but a time-dependent covariate, which jumps every unit of time on $[0, 10]$. We simulated this covariate by drawing 11 independent random uniform variables, and by accumulating successively these variables. This resulted in a positive step-wise constant increasing covariate, which sizes of jumps are uniformly distributed. We divided this covariate by 11, the number of constant steps, so that the covariate values remain between 0 and 1. We chose to do so because of the way the covariate values are integrated into the failure intensity: without dividing the simulated covariate, we would get a maximum value of $\exp(\gamma_0' \mathbb{X}_{10}^{(\max)}) = \exp(11) \simeq 60000$, with a mean of $(\exp(11) - 1)/11 \simeq 5400$. These potential values, which appear as a factor of the failure intensity, would make impossible to distinguish any information from the virtual age model itself. Rather than changing the order of magnitude of γ_0, we chose to normalize the covariate. We simulated the datasets with the first method exposed in 2.2.2.

Heatmaps of the empirical MSE obtained in this setting are given in Figure 8, which reads just as Figure 5.

General results. In comparison with the case of constant covariates, we find here patterns in the heatmaps quite similar, except for γ, the coefficient of the covariates, which has no more a random look. The values of the MSE are almost the same for β and ρ. They are multiplied by 2 (ARA models) or 4 (QR model) for η, and by 8 (ARA models) or 37 (QR model) for γ. It must be noticed that η and γ have a close link in the model: in the case of a constant covariate, both have a multiplicative effect (*via* a reparametrization for η) on the conditionnal intensity. We see here that the introduction of a time-dependent covariate in the model disturbs the quality of estimation of both parameters. However, except for some

high values for γ in the QR model, the MSE stay reasonably low.

Influence of the parameters. For β, we find again, as already said, that the higher ρ_0 is and the lower β_0 is, the better the estimations are. The biases are under 0.02 for the ARA models and 0.1 for the QR model.

We find a slightly clearer influence of ρ_0 on the quality of estimation of η: the higher it is, the lower the MSE are. At a first glance, we could say that this influence is the same for β_0, but it must be noticed that it is not true for low values of ρ_0 within the QR model. The relative biases with respect to the true value are under 1 % for the ARA models and under 19 % for the QR model, with much lower values when ρ_0 is high.

For ρ, we get almost the same heatmaps as in the constant covariate case, with only slightly higher values within the ARA models.

The case of γ, the coefficient of the covariate, is the most interesting. This time, there is an influence of both β_0 and ρ_0 on the quality of estimation of γ. It looks like for all models, the higher ρ_0 is, the better the estimations are, even though it is not true for $\rho_0 \leq 0.7$ within the QR model. In contrast, the effect of β_0 is not the same for all models. Within the ARA models, the higher it is, the lower the MSE are, especially for high values of β_0. The pattern for low values of ρ_0 is rather unclear. Within the QR model, it is clear that the lower β_0 is, the better the estimations of γ are. In the ARA_∞ model, γ is generally underestimated, with a bias up to 0.027. On the contrary, γ is overestimated within the QR model, with biases up to 0.66. With respect to the true value $\gamma_0 = 1$, these are quite high values. Within the ARA_1 model, we find that γ is overestimated with a bias up to 0.012 when β_0 is high and ρ_0 is low, and is underestimated with a bias up to 0.0057 when β_0 is low and ρ_0 is high. With the latter configuration, which means that the systems wear slowly and that the repairs are very efficient, the conditional failure intensity globally increases slowly. Therefore, the failure times are more spaced. Within the estimation procedure, this could be understood as a low impact of the covariate (which is positive), leading to an underestimation of γ. The reverse is true for the former configuration.

3.2.2. Influence of the coefficient of the covariate

We focus here on the influence of γ_0 on the quality of estimation. Only the case $\beta_0 = 2.5$, $\rho_0 = 0.7$ for the ARA models and $\rho_0 = 0.9$ for the QR model was considered while γ_0 varied in the set $\{-3, -2, \ldots, 3\}$. η_0 was chosen according to the procedure already explained. Plots of the empirical MSE obtained in this setting are given in Figure 9.

The results here are very different from the constant covariate case. For β, there is no influence of γ_0 on the estimations within the ARA_∞ and the QR models. In contrast, the higher γ_0 is, the higher the MSE are within the ARA_1 model. For the three models, the biases are constant. The variation that occurs for ARA_1 therefore comes from the standard deviation, which shows the same phenomenon. However, for the three models, the values have the same order of magnitude as in the constant covariate case. We observe the same thing in the estimation of η, except that it is here the QR model that shows the highest values. We cannot directly compare the values, since we were talking of non normalized MSE in the case of a constant covariate, whereas here we had to normalize the MSE by

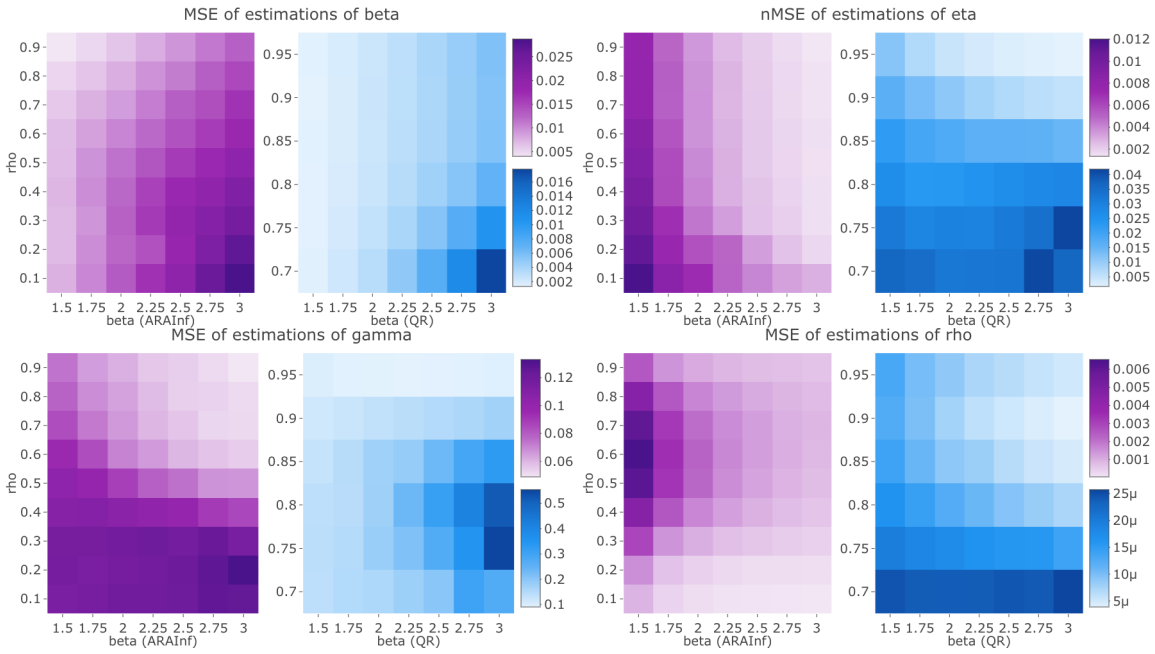

Figure 8: MSE of the estimations of the four parameters in the case of a time-dependent covariate, versus the true values of β_0 and ρ_0

the varying true value η_0. If we normalize the latter, we find values of the same order of magnitude as the former. Regarding ρ, the situation is the same as for β, with an increase of the MSE within the ARA_1 model with higher values of γ_0, that is also observable on the standard deviations. The order of magnitude is the same as in the constant covariate case. The look of the plot for the estimations of γ is totally different from the constant covariate case. Here, the curves for the ARA models show a constant behavior, either for the MSE, the bias, or the standard deviation. The bias is never more than 0.017, which is a low value with respect to the true value $\gamma_0 = 1$. The standard deviation is up to 0.44 for the ARA_1 model, and to 0.27 for the ARA_∞ model. Then, we see that the higher γ_0 is, the higher the MSE are within the QR model. This comes as well from the standard deviation, which exhibits the same monotonicity, as from the bias, which increases when γ_0 is high. In fact, γ is more and more underestimated, with a bias of up to 0.22.

3.2.3. Influence of data size on the quality of estimation

Settings. This part of the numerical study intends to analyse how the dimensions of the datasets influence the quality of estimation. We allowed again the number of systems ν and the number of failures per system n to vary in the set $\{5, 10, 15, \ldots, 50\}$. We chose the ARA_∞ model to study two different types of covariate. In order to focus on the data size, we chose the model parameters among ones that showed good results: $\eta_0 = 1/(0.1^{1/2.5})$, $\beta_0 = 2.5$, $\rho_0 = 0.7$, $\gamma_0 = 1$. For each pair of ν and n, we simulated $M = 10000$ datasets.

The time-dependent covariate was simulated either as previously as the normalized cumulative sum of 11 uniform random variables (and is therefore increasing with time), or as

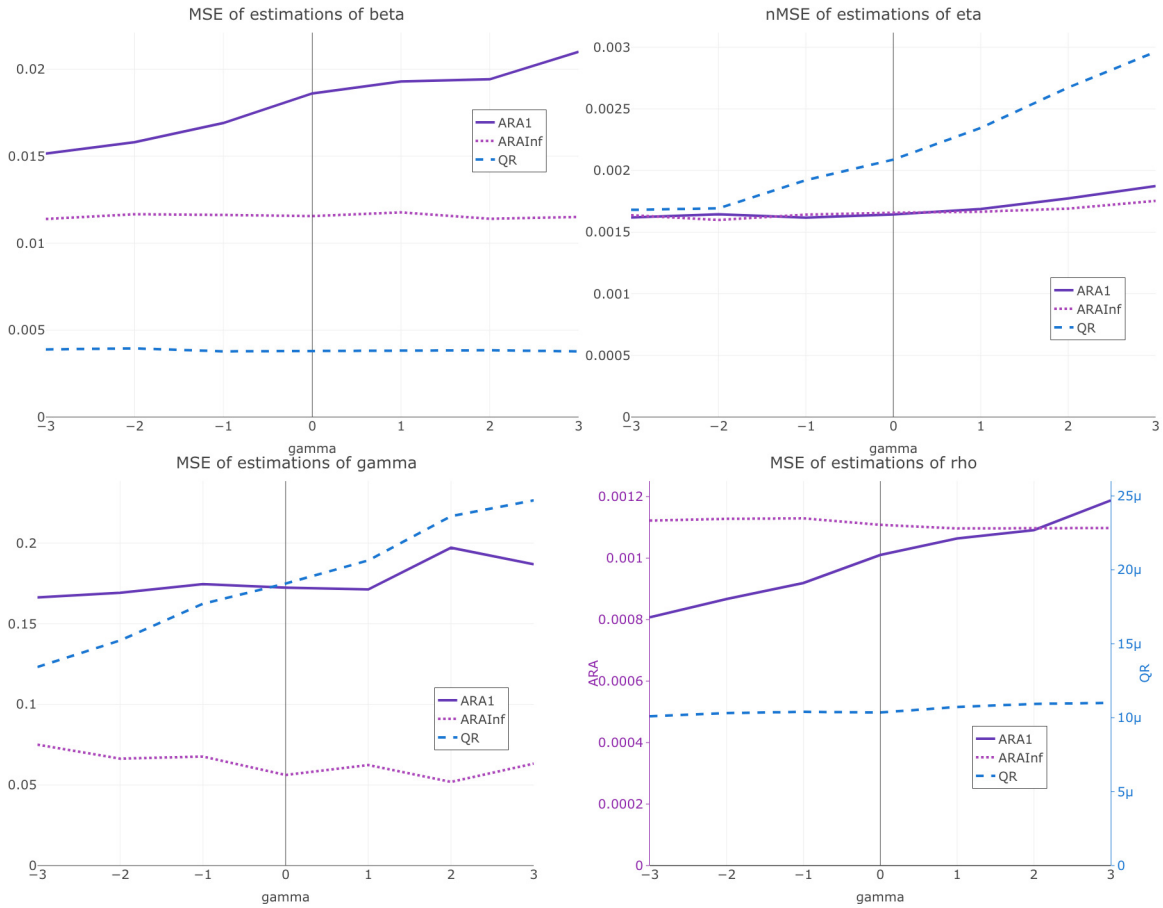

Figure 9: MSE of the estimations of the four parameters in the case of a time-dependent covariate, versus the true values of γ_0

a random variable taking its values within the set $\{-2, -1, 0, 1, 2\}$, jumping from a value to an adjacent one at times $1, 2, \ldots, 10$. We have set probabilities of the following type: at point -2, the probability to jump in -1 is 1; at point -1, the probability to jump in -2 is 0.5 and the probability to jump in 0 is 0.5, *etc.* A graphical summary of these probabilities is given in Figure 3.2.3. The initial state is always 0.

Heatmaps. Heatmaps of the empirical MSE obtained in this setting are given in Figure 11, which reads just as Figure 7, apart from the fact that the graphs for the ARA_∞ model are replaced with the graphs for the increasing covariate and the graphs for the QR model are replaced with the graphs for the finite state space covariate. Again, we see a clear trend to get better estimations when the data size increases, either in terms of number of systems or of number of failures, which is what we expected. Except for γ, the scales are comparable and even a little smaller than in the constant covariate case. It seems that for small samples, it works better for time-dependent covariates.

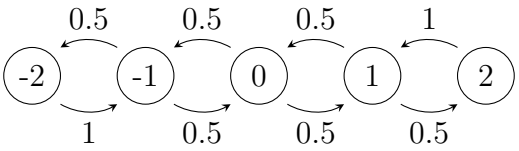

Figure 10: Probabilities of jumping from one state to another for the time-dependent covariate

Parameters of the Weibull distribution. We observe here the same phenomenon as for a constant covariate: it is easier to estimate β and η, respectively the shape and the scale parameters of the initial intensity, with more systems rather than with more failures per system. The biases are rather symmetric, and show that these two parameters are generally overestimated. However, this overestimation decreases quickly with more data. The standard deviations are not symmetric, and exhibit the same trend as the MSE.

Efficiency of the maintenances. Again, as in the case of the ARA_∞ model with a constant covariate, ρ is easier to estimate with more systems rather than with more failures per system. We already gave a potential reason for that: the three other parameters are more easily estimated with more systems, which may impact the quality of estimation of ρ, although this parameter represents the efficiency of the maintenances. The biases may reveal even more clearly this phenomenon: with only 5 systems per dataset, the biases reach 0.018, whatever the number of failures is, whereas with 10 systems, they never hit 0.010. In any case, these biases are reasonably low, and show only a slight underestimation of ρ.

Coefficient of the covariate. Finally, we observe that in the case of the non monotonic covariate, as expected, it is easier to estimate γ when there are more systems. However, in the case of the cumulative uniform covariate, it is the opposite: more failures per system provide a better estimation than more systems per dataset. Regarding the biases, it is interesting to notice that with the cumulative uniform covariate, γ tends to be underestimated (bias of 0.39 for a 5×5 dataset, only 0.15 for a 5×10 or 10×5 dataset) whereas with the finite state space covariate, it is slightly overestimated (bias of 0.095 for a 5×5 dataset, only 0.050 for a 5×10 or 10×5 dataset).

4. Conclusion

4.1. Main results

This paper proposed a parametric model able to take into account the intrinsic wear, the effect of imperfect maintenances and the heterogeneity of several almost identical and independent systems. It set up a mathematical framework and developed two simulation methods as well as the estimation of the model parameters.

The other achievement of this article was to assess the quality of estimation. We found that when estimating the virtual age model parameters along with the coefficient of influence of constant covariates, the results are satisfyingly good. They look close to those we obtained without covariate in terms of MSE. The influence of the different parameters simulation

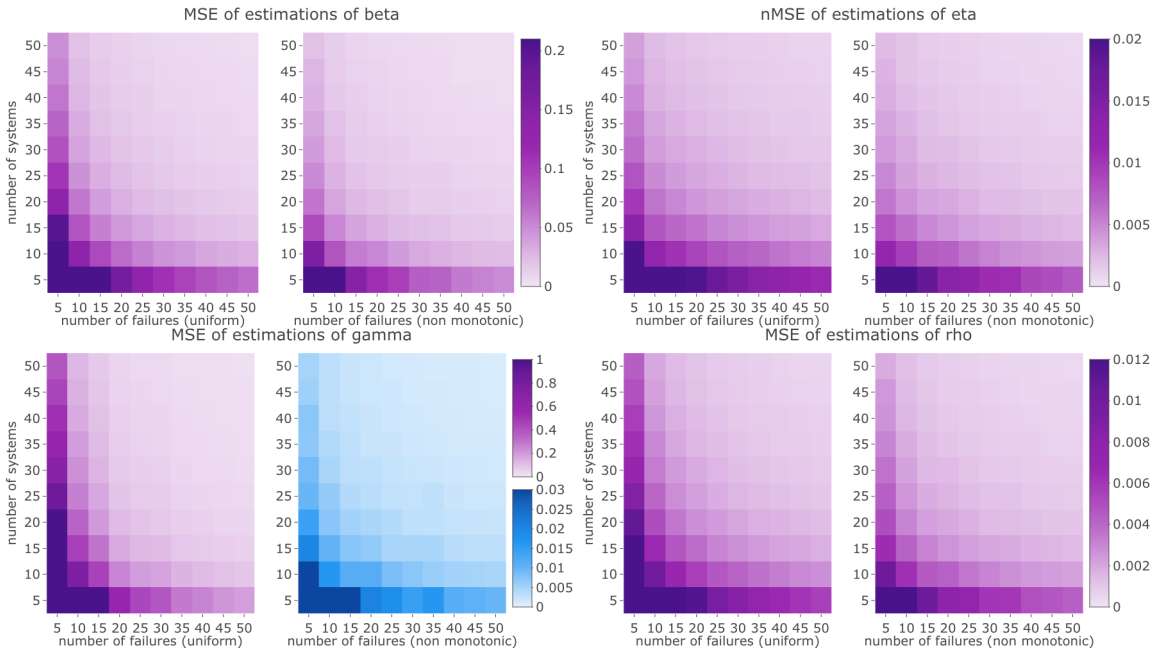

Figure 11: MSE of the estimations of the four parameters in the case of a time-dependent covariate, versus the number n of failures per system and the number ν of systems per dataset

values on the quality of estimation has been carefully studied. In particular, we empirically found that the intrinsic wear rate of the systems and the efficiency of the maintenances have no influence on the quality of estimation of the covariates coefficient, and converselyin the case of a constant covariate. Regarding the covariates coefficient, some interesting questions were raised: the quality for this coefficient is symmetrical whether its simulation value is negative or positive. Moreover, the quality increases when the simulation value is high, with a quadratic-like growth. Finally, the three studied models exhibit the same quality of estimation for a null coefficient. This may lead to future work in order to derive theoretical properties on the estimators. The quality of estimation with time-dependent covariates was found to be not as good as in the constant covariate case, but it remains quite satisfying. We observed different patterns when considering the quality with respect to the model parameters. In particular, whereas the coefficient of the constant covariate had no influence on the quality of estimation of the other parameters, it has some when the covariate is time-dependent.

Regarding the influence of data size, we fortunately found that the more data we have, the better the estimation is. We highlighted the fact that the behaviour of the estimators is not symmetrical whether it is the number of systems that increases, or the number of failures per system. First, the more systems we have, the easier it is to estimate the parameters of the intrinsic wear of the systems: indeed, these parameters are best estimated when we observe a large number of first failure times. After repairs, the information tends to be blurred by the effect of the maintenances, that is simultaneously estimated. Second, the reverse is true for QR and easily understandable: the more successive maintenances we have, the better the

efficiency can be estimated. Third, the estimation of the covariates influence is less precise with small datasets. The more systems we have, the better it is, since for a single system, this coefficient is undistinguishable from the scale of the baseline hazard rate. Each system corresponds to a single value of the covariates. Therefore, the amount of information is too small to perform a good estimation.

4.2. Future work

The good results of the estimation procedure should be examined to understand what are the underlying mathematical properties of the estimators. We also empirically highlighted some interesting features with the influence of the coefficient of the covariate on the quality of estimation. Some mathematical properties may be derived from these characteristics. Another extension could be the evaluation of the influence of the covariate sampling on the quality of estimation. For example, one may not record all the jumps of a time-dependent covariate. The impact of this sampling should be assessed. Such a work could lead to study a continuous covariate that is a degradation process, recorded at some predefined times. Peng *et al.* [10] did study an imperfect maintenance model with a stochastic process as a covariate, but it was in a Bayesian framework.

Acknowledgements

This work has been partially supported by the LabEx PERSYVAL-Lab (ANR-11-LABX-0025-01) funded by the French program Investissement davenir.

Most of the computations presented in this paper were performed using the GRICAD infrastructure (https://gricad.univ-grenoble-alpes.fr), which is partly supported by the Equip@Meso project (reference ANR-10-EQPX-29-01) of the programme Investissements d'Avenir supervised by the Agence Nationale pour la Recherche.

Appendix A. Detailed computations for the simulation of failure times

With the hypothesis set in Section 2.2, the conditional cumulative distribution function is decomposed along the discontinuity points of the covariates in Equation (13). There are three cases: 1. When $l_{(T_i)} = l_{(t)}$, which is represented in Figure A.12, the computation is as follows:

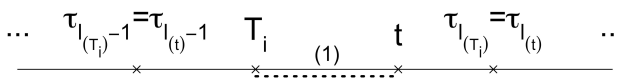

Figure A.12: First case occurring when computing the cumulative distribution function.

$$\boldsymbol{f} = \overbrace{g_{l_{(T_i)}} \int_{T_i}^{t} V_i'(s) h(V_i(s)) ds}^{(1)} = g_{l_{(T_i)}} \left(H(V_i(t)) - H(V_i(T_i)) \right). \tag{A.1}$$

2. When $l_{(T_i)} = l_{(t)} - 1$, which is represented in Figure A.13, the computation is as follows:

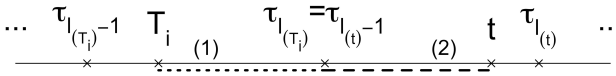

Figure A.13: Second case occurring when computing the cumulative distribution function.

$$\begin{aligned}\boldsymbol{f} &= \overbrace{g_{l_{(T_i)}} \int_{T_i}^{\tau_{l_{(T_i)}}} V_i'(s)h(V_i(s))ds}^{(1)} + \overbrace{g_{l_{(t)}} \int_{\tau_{l_{(t)}-1}}^{t} V_i'(s)h(V_i(s))ds}^{(2)} \\ &= g_{l_{(T_i)}} \Big(H(V_i(\tau_{l_{(T_i)}})) - H(V_i(T_i)) \Big) + g_{l_{(t)}} \Big(H(V_i(t)) - H(V_i(\tau_{l_{(t)}-1})) \Big). \end{aligned} \tag{A.2}$$

3. When $l_{(T_i)} \leq l_{(t)} - 2$, which is represented in Figure A.14, the computation is as follows:

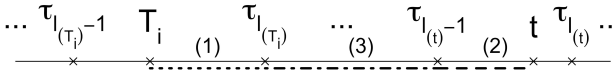

Figure A.14: Third case occurring when computing the cumulative distribution function.

$$\begin{aligned}\boldsymbol{f} &= \overbrace{\sum_{l=l_{(T_i)}+1}^{l_{(t)}-1} g_l \int_{\tau_{l-1}}^{\tau_l} V_i'(s)h(V_i(s))ds}^{(3)} + \overbrace{g_{l_{(T_i)}} \int_{T_i}^{\tau_{l_{(T_i)}}} V_i'(s)h(V_i(s))ds}^{(1)} + \overbrace{g_{l_{(t)}} \int_{\tau_{l_{(t)}-1}}^{t} V_i'(s)h(V_i(s))ds}^{(2)} \\ &= \sum_{l=l_{(T_i)}+1}^{l_{(t)}-1} g_l \left(H(V_i(\tau_l)) - H(V_i(\tau_{l-1})) \right) \\ &\qquad + g_{l_{(T_i)}} \Big(H(V_i(\tau_{l_{(T_i)}})) - H(V_i(T_i)) \Big) + g_{l_{(t)}} \Big(H(V_i(t)) - H(V_i(\tau_{l_{(t)}-1})) \Big). \end{aligned} \tag{A.3}$$

Therefore, if $l_{(T_i)} = l_{(t)}$,

$$F_{i+1}(t) = 1 - \exp\Big(- g_{l_{(T_i)}} \left(H(V_i(t)) - H(V_i(T_i)) \right) \Big). \tag{A.4}$$

Else,

$$\begin{aligned} F_{i+1}(t) = 1 - \exp\Bigg(&- \sum_{l=l_{(T_i)}+1}^{l_{(t)}-1} g_l \big(H(V_i(\tau_l)) - H(V_i(\tau_{l-1})) \big) \\ &- g_{l_{(T_i)}} \big(H(V_i(\tau_{l_{(T_i)}})) - H(V_i(T_i)) \big) - g_{l_{(t)}} \big(H(V_i(t)) - H(V_i(\tau_{l_{(t)}-1})) \big) \Bigg), \end{aligned} \tag{A.5}$$

with $g_l := \exp(\gamma' \chi_l)$, and the sum being eventually empty if $l_{(T_i)} = l_{(t)} - 1$.

References

[1] M. Kijima, Some results for repairable systems with general repair, J. Appl. probab. 26 (1) (1989) 89–102. doi:10.2307/3214319.

[2] L. Doyen, O. Gaudoin, Classes of imperfect repair models based on reduction of failure intensity or virtual age, Reliab. Eng. Syst. Saf. 84 (1) (2004) 45–56. doi:10.1016/S0951-8320(03)00173-X.

[3] L. Doyen, R. Drouilhet, L. Brenière, A generic framework for generalized virtual age models, IEEE Trans. Reliab. (to appear). doi:10.1109/TR.2019.2906732.

[4] H. Wang, H. Pham, A quasi renewal process and its applications in imperfect maintenance, Int. j. syst. sci. 27 (10) (1996) 1055–1062. doi:10.1080/00207729608929311.

[5] C. Chauvel, J.-Y. Dauxois, L. Doyen, O. Gaudoin, Parametric bootstrap goodness-of-fit tests for imperfect maintenance models, IEEE Trans. Reliab. 65 (3) (2016) 1343–1359. doi:10.1109/TR.2016.2578938.

[6] J.-Y. Dauxois, E. Maalouf, Statistical inference in a model of imperfect maintenance with arithmetic reduction of intensity, IEEE Trans. Reliab. 67 (3) (2018) 987–997. doi:10.1109/TR.2018.2828331.

[7] J.-Y. Dauxois, S. Gasmi, O. Gaudoin, Semiparametric inference for an extended geometric failure rate reduction model, J. Stat. Plan. Inference 199 (2019) 14–28. doi:10.1016/j.jspi.2018.05.002.

[8] Y. Dijoux, M. Fouladirad, D. T. Nguyen, Statistical inference for imperfect maintenance models with missing data, Reliab. Eng. Syst. Saf. 154 (2016) 84–96. doi:10.1016/j.ress.2016.05.017.

[9] L. Doyen, O. Gaudoin, A. Syamsundar, On geometric reduction of age or intensity models for imperfect maintenance, Reliab. Eng. Syst. Saf. 168 (2017) 40–52. doi:10.1016/j.ress.2017.03.015.

[10] W. Peng, L. Shen, Y. Shen, Q. Sun, Reliability analysis of repairable systems with recurrent misuse-induced failures and normal-operation failures, Reliab. Eng. Syst. Saf. 171 (2018) 87–98. doi:10.1016/j.ress.2017.11.016.

[11] L. Peng, B. Liu, L. Ma, N. Wang, Q. Liu, Mixed arithmetic reduction model for two-unit system maintenance, in: 2017 Second International Conference on Reliability Systems Engineering (ICRSE), IEEE, 2017, pp. 1–8. doi:10.1109/ICRSE.2017.8030798.

[12] U. Said, S. Taghipour, Modeling failure process and quantifying the effects of multiple types of preventive maintenance for a repairable system, Qual. Reliab. Eng. Int. 33 (5) (2017) 1149–1161. doi:10.1002/qre.2088.

[13] G. Salles, S. Mercier, L. Bordes, Semiparametric estimate of the efficiency of imperfect maintenance actions for a gamma deteriorating system, J. Stat. Plan. Inference 206 (2020) 278–297. doi:10.1016/j.jspi.2019.09.014.

[14] J. Hu, J. Shen, L. Shen, Periodic preventive maintenance planning for systems working under a markovian operating condition, Comput. Ind. Eng. 142 (2020) 106291. doi:10.1016/j.cie.2020.106291.

[15] K. T. Huynh, A hybrid condition-based maintenance model for deteriorating systems subject to nonmemoryless imperfect repairs and perfect replacements, IEEE Trans. Reliab.doi:10.1109/TR.2019.2942019.

[16] S. Mercier, I. T. Castro, Stochastic comparisons of imperfect maintenance models for a gamma deteriorating system, Eur. J. Oper. Res. 273 (1) (2019) 237–248. doi:10.1016/j.ejor.2018.06.020.

[17] R. Mullor, J. Mulero, M. Trottini, A modelling approach to optimal imperfect maintenance of repairable equipment with multiple failure modes, Comput. Ind. Eng. 128 (2019) 24–31. doi:10.1016/j.cie.2018.12.032.

[18] L. Yang, Z.-s. Ye, C.-G. Lee, S.-f. Yang, R. Peng, A two-phase preventive maintenance policy considering imperfect repair and postponed replacement, Eur. J. Oper. Res. 274 (3) (2019) 966–977. doi:10.1016/j.ejor.2018.10.049.

[19] M. Aramesh, M. Attia, H. Kishawy, M. Balazinski, Estimating the remaining useful tool life of worn tools under different cutting parameters: A survival life analysis during turning of titanium metal matrix composites (ti-mmcs), CIRP J. Manuf. Sci. Technol. 12 (2016) 35–43. doi:10.1016/j.cirpj.2015.10.001.

[20] J. Man, Q. Zhou, Prediction of hard failures with stochastic degradation signals using wiener process and proportional hazards model, Comput. Ind. Eng. 125 (2018) 480–489. doi:10.1016/j.cie.2018.09.015.

[21] J. Man, Q. Zhou, Remaining useful life prediction for hard failures using joint model with extended hazard, Qual. Reliab. Eng. Int. 34 (5) (2018) 748–758. doi:10.1002/qre.2285.

[22] R. Bender, T. Augustin, M. Blettner, Generating survival times to simulate cox proportional hazards models, Stat. med. 24 (11) (2005) 1713–1723. doi:10.1002/sim.2059.
[23] L. D. Fisher, D. Y. Lin, Time-dependent covariates in the cox proportional-hazards regression model, Annu. rev. public health 20 (1) (1999) 145–157. doi:10.1146/annurev.publhealth.20.1.145.
[24] Q. Zhou, J. Son, S. Zhou, X. Mao, M. Salman, Remaining useful life prediction of individual units subject to hard failure, IIE Trans. 46 (10) (2014) 1017–1030. doi:10.1080/0740817X.2013.876126.
[25] X. Liu, R. Pan, Analysis of large heterogeneous repairable system reliability data with static system attributes and dynamic sensor measurement in big data environment, Technometrics (2019) 1–34doi:10.1080/00401706.2019.1609584.
[26] J. Fosen, Ø. Borgan, H. Weedon-Fekjær, O. O. Aalen, Dynamic analysis of recurrent event data using the additive hazard model, Biom. J.: J. Math. Methods Biosci. 48 (3) (2006) 381–398. doi:10.1002/bimj.200510217.
[27] X. Zhao, L. Liu, Y. Liu, W. Xu, Analysis of multivariate recurrent event data with time-dependent covariates and informative censoring, Biom. j. 54 (5) (2012) 585–599. doi:10.1002/bimj.201100194.
[28] M. Giorgio, M. Guida, G. Pulcini, Repairable system analysis in presence of covariates and random effects, Reliab. Eng. Syst. Saf. 131 (2014) 271–281. doi:10.1016/j.ress.2014.04.009.
[29] P. Novák, Regression models for repairable systems, Methodol. Comput. Appl. Probab. 17 (4) (2015) 963–972. doi:10.1007/s11009-014-9419-2.
[30] S. Li, Y. Sun, C.-Y. Huang, D. A. Follmann, R. Krause, Recurrent event data analysis with intermittently observed time-varying covariates, Stat. med. 35 (18) (2016) 3049–3065. doi:10.1002/sim.6901.
[31] H. He, D. Pan, L. Sun, Y. Li, L. L. Robison, X. Song, Analysis of a fixed center effect additive rates model for recurrent event data, Comput. Stat. Data Anal. 112 (2017) 186–197. doi:10.1016/j.csda.2017.03.003.
[32] P. Maitra, L. D. A. F. A. Amorim, J. Cai, Multiplicative rates model for recurrent events in case-cohort studies, Lifetime Data Anal. 26 (1) (2020) 134–157. doi:10.1007/s10985-019-09466-0.
[33] J. Ning, C. Cai, Y. Chen, X. Huang, M.-C. Wang, Semiparametric modelling and estimation of covariate-adjusted dependence between bivariate recurrent events, Biometricsdoi:10.1111/biom.13229.
[34] G. Xu, S. H. Chiou, C.-Y. Huang, M.-C. Wang, J. Yan, Joint scale-change models for recurrent events and failure time, J. Am. Stat. Assoc. 112 (518) (2017) 794–805. doi:10.1080/01621459.2016.1173557.
[35] P. K. Andersen, J. Angst, H. Ravn, Modeling marginal features in studies of recurrent events in the presence of a terminal event, Lifetime data anal. 25 (4) (2019) 681–695. doi:10.1007/s10985-019-09462-4.
[36] M. Han, L. Sun, Y. Liu, J. Zhu, Joint analysis of recurrent event data with additive–multiplicative hazards model for the terminal event time, Metrika 81 (5) (2018) 523–547. doi:10.1007/s00184-018-0654-3.
[37] D. Han, X. Su, L. Sun, Z. Zhang, L. Liu, Variable selection in joint frailty models of recurrent and terminal events, Biometricsdoi:10.1111/biom.13242.
[38] Y.-J. Kim, Joint model for recurrent event data with a cured fraction and a terminal event, Biom. J.doi:10.1002/bimj.201800321.
[39] X. Sun, J. Ding, L. Sun, A semiparametric additive rates model for the weighted composite endpoint of recurrent and terminal events, Lifetime data anal. (2019) 1–22doi:10.1007/s10985-019-09486-w.
[40] A. Deep, D. Veeramani, S. Zhou, Event prediction for individual unit based on recurrent event data collected in teleservice systems, IEEE Trans. Reliab.doi:10.1109/TR.2019.2909471.
[41] C. H. Lee, C.-Y. Huang, G. Xu, X. Luo, Semiparametric regression analysis for alternating recurrent event data, Stat. med. 37 (6) (2018) 996–1008. doi:10.1002/sim.7563.
[42] L.-A. Lin, S. Luo, B. R. Davis, Bayesian regression model for recurrent event data with event-varying covariate effects and event effect, J. appl. stat. 45 (7) (2018) 1260–1276. doi:10.1080/02664763.2017.1367368.
[43] V. Slimáček, B. H. Lindqvist, Nonhomogeneous poisson process with nonparametric frailty and covariates, Reliab. Eng. Syst. Saf. 167 (2017) 75–83. doi:10.1016/j.ress.2017.05.026.
[44] M. Akacha, E. O. Ogundimu, Sensitivity analyses for partially observed recurrent event data, Pharm. stat. 15 (1) (2016) 4–14. doi:10.1002/pst.1720.

[45] S. Wu, P. Scarf, Decline and repair, and covariate effects, Eur. J. Oper. Res. 244 (1) (2015) 219–226. doi:10.1016/j.ejor.2015.01.041.
[46] E. A. Peña, Asymptotics for a class of dynamic recurrent event models, J. nonparametric stat. 28 (4) (2016) 716–735. doi:0.1080/10485252.2016.1225733.
[47] A. Syamsundar, V. N. A. Naikan, Imperfect repair proportional intensity models for maintained systems, IEEE Trans. Reliab. 60 (4) (2011) 782–787. doi:10.1109/TR.2011.2161110.
[48] K. Claudio, V. Couallier, Y. Le Gat, Integration of time-dependent covariates in recurrent events modelling: application to failures on drinking water networks, J. Soc. Fr. Stat. 155 (3) (2014) 62–77.
[49] L. Li, T. E. Hanson, A bayesian semiparametric regression model for reliability data using effective age, Comput. Stat. Data Anal. 73 (2014) 177–188. doi:10.1016/j.csda.2013.11.015.
[50] L. Brenière, L. Doyen, C. Bérenguer, Simulation and Parameter Estimation for Virtual Age Models with Time-Dependent Covariates: Methodology and Performance Evaluation, in: Proc. 29th Eur. Saf. Reliab. Conf. - ESREL 2019, Hannover, Germany, 2019, pp. 1025–1032. doi:10.3850/978-981-11-2724-3_0191-cd.
[51] D. R. Cox, Regression models and life-tables, J. Royal Stat. Soc.: Ser. B (Methodol.) 34 (2) (1972) 187–202. doi:10.1111/j.2517-6161.1972.tb00899.x.
[52] L. Yeh, Nonparametric inference for geometric processes, Commun. stat. - theory methods 21 (7) (1992) 2083–2105. doi:10.1080/03610929208830899.
[53] J. A. Nelder, R. Mead, A Simplex Method for Function Minimization, Comput. J. 7 (4) (1965) 308–313. doi:10.1093/comjnl/7.4.308.